Article
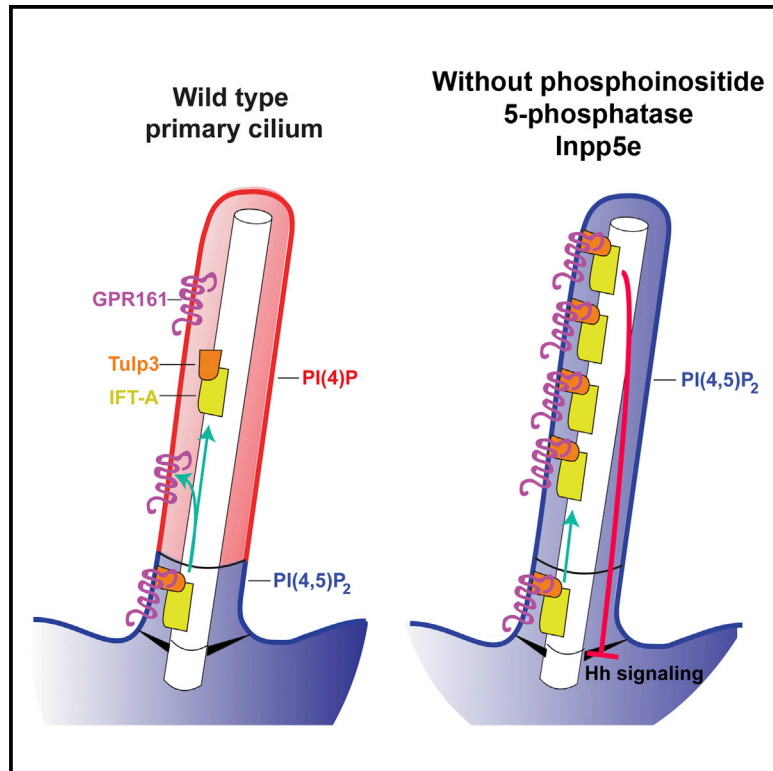
Phosphoinositides Regulate Ciliary Protein Trafficking to Modulate Hedgehog Signaling

Graphical Abstract

Authors

Francesc R. Garcia-Gonzalo, Siew Cheng Phua, Elle C. Roberson, ..., Stéphane Schurmans, Takanari Inoue, Jeremy F. Reiter

Correspondence

jctinoue@jhmi.edu (T.I.), jeremy.reiter@ucsf.edu (J.F.R.)

In Brief

Garcia-Gonzalo et al. show that different domains of the ciliary membrane contain different phosphoinositides. The ciliopathy-associated enzyme Inpp5e controls this distribution, which is needed for trafficking of ciliary proteins, including Hedgehog signaling regulators Tulp3 and Gpr161. Disrupting phosphoinositide distribution impacts Hedgehog signaling, suggesting lipids are critical components of the cilia signaling environment.

Highlights

- The ciliary membrane contains different phosphoinositides than that of its base

- The ciliopathy-associated protein Inpp5e generates the phosphoinositide distribution

- Ciliary phosphoinositides are required for normal Hedgehog (Hh) signaling

- Tulp3 senses phosphoinositides to limit ciliary Gpr161, an inhibitor of Hh signaling

CellPress

Phosphoinositides Regulate Ciliary Protein Trafficking to Modulate Hedgehog Signaling

Francesc R. Garcia-Gonzalo,[1,4] Siew Cheng Phua,[2,4] Elle C. Roberson,[1] Galo Garcia III,[1] Monika Abedin,[1]
Stéphane Schurmans,[3] Takanari Inoue,[2,*] and Jeremy F. Reiter[1,*]
[1]Department of Biochemistry and Biophysics and Cardiovascular Research Institute, University of California, San Francisco, San Francisco, CA 94158, USA
[2]Department of Cell Biology and Center for Cell Dynamics, Johns Hopkins University School of Medicine, Baltimore, MD 21205, USA
[3]Laboratory of Functional Genetics, GIGA-Research Centre, Université de Liège, 4000-Liège, Belgium
[4]Co-first author
*Correspondence: jctinoue@jhmi.edu (T.I.), jeremy.reiter@ucsf.edu (J.F.R.)
http://dx.doi.org/10.1016/j.devcel.2015.08.001

SUMMARY

Primary cilia interpret vertebrate Hedgehog (Hh) signals. Why cilia are essential for signaling is unclear. One possibility is that some forms of signaling require a distinct membrane lipid composition, found at cilia. We found that the ciliary membrane contains a particular phosphoinositide, PI(4)P, whereas a different phosphoinositide, $PI(4,5)P_2$, is restricted to the membrane of the ciliary base. This distribution is created by Inpp5e, a ciliary phosphoinositide 5-phosphatase. Without Inpp5e, ciliary $PI(4,5)P_2$ levels are elevated and Hh signaling is disrupted. Inpp5e limits the ciliary levels of inhibitors of Hh signaling, including Gpr161 and the $PI(4,5)P_2$-binding protein Tulp3. Increasing ciliary $PI(4,5)P_2$ levels or conferring the ability to bind PI(4)P on Tulp3 increases the ciliary localization of Tulp3. Lowering Tulp3 in cells lacking Inpp5e reduces ciliary Gpr161 levels and restores Hh signaling. Therefore, Inpp5e regulates ciliary membrane phosphoinositide composition, and Tulp3 reads out ciliary phosphoinositides to control ciliary protein localization, enabling Hh signaling.

INTRODUCTION

Primary cilia are sensory organelles whose malfunction causes human diseases, known as ciliopathies (Hildebrandt et al., 2011). Cilia are also required to interpret vertebrate Hedgehog (Hh) signals, patterning cues vital for embryonic development and adult tissue homeostasis (Goetz and Anderson, 2010). How cilia transduce Hh signals is imperfectly understood, but it involves the coordinated trafficking of proteins into and out of cilia. In the absence of Hh signals, such as Sonic hedgehog (Shh), the G protein-coupled receptor (GPCR) Gpr161 localizes to cilia and keeps the downstream Gli transcription factors in their repressor forms (Mukhopadhyay et al., 2013). Binding of Shh to its receptor Patched1 (Ptch1) causes the ciliary accumulation of Smoothened (Smo) and the ciliary exit of Gpr161, thereby inducing the activation of Gli transcription factors,

which move from the cilium to the nucleus and induce the Hh transcriptional program. Ciliary localization of Gpr161 requires a ciliary trafficking complex that includes Tulp3 and the intraflagellar transport complex A (IFT-A) (Mukhopadhyay et al., 2010, 2013; Norman et al., 2009; Patterson et al., 2009; Cameron et al., 2009; Qin et al., 2011; Tran et al., 2008; Liem et al., 2012).

Although it is clear that the protein composition of the ciliary membrane is distinct from that of the surrounding, contiguous plasma membrane, it has been less clear how the lipid composition of the ciliary membrane differs from that of other cellular membranes. In Paramecia, the ciliary membrane is enriched in sphingolipids, and a mutation that alters ciliary lipid composition affects ciliary channel activity, suggesting that the ciliary lipid composition is critical for its function (Kaneshiro et al., 1984; Andrews and Nelson, 1979; Forte et al., 1981). Similarly, in Tetrahymena and Chlamydomonas, certain lipids are enriched in their cilia or flagella (Kennedy and Thompson, 1970; Jonah and Erwin, 1971; Smith et al., 1970; Gealt et al., 1981; Bloodgood et al., 1985). In Trypanosomes, the flagellum possesses high levels of sterols and saturated fatty acids and shows a high degree of lipid organization (Tyler et al., 2009; Souto-Padrón and de Souza, 1983). A region of high lipid organization also exists at the base of vertebrate epithelial cilia, indicating that subdomains within the cilium may differ in their lipid composition (Vieira et al., 2006; Montesano, 1979).

Different forms of another class of lipids, the phosphoinositides, help to define different cellular membranes (Di Paolo and De Camilli, 2006; Roth, 2004; Sasaki et al., 2009). In *C. elegans*, a phosphoinositide 5-phosphatase, CIL-1, controls PI(3)P levels and the ciliary localization of PKD-2, suggesting that phosphoinositides can participate in ciliary protein trafficking (Bae et al., 2009). In mammals, three phosphoinositide 5-phosphatases—Ocrl, Inpp5b, and Inpp5e—can localize to cilia (Jacoby et al., 2009; Bielas et al., 2009; Luo et al., 2012, 2013). Mutations in human *INPP5E* can cause the ciliopathy Joubert syndrome, and knockout of mouse *Inpp5e* results in phenotypes characteristic of ciliopathies, including cystic kidneys and polydactyly (Jacoby et al., 2009; Bielas et al., 2009). Therefore, we investigated whether distinct phosphoinositides were present in the ciliary membrane and whether they participate in the unique signaling functions of vertebrate cilia.
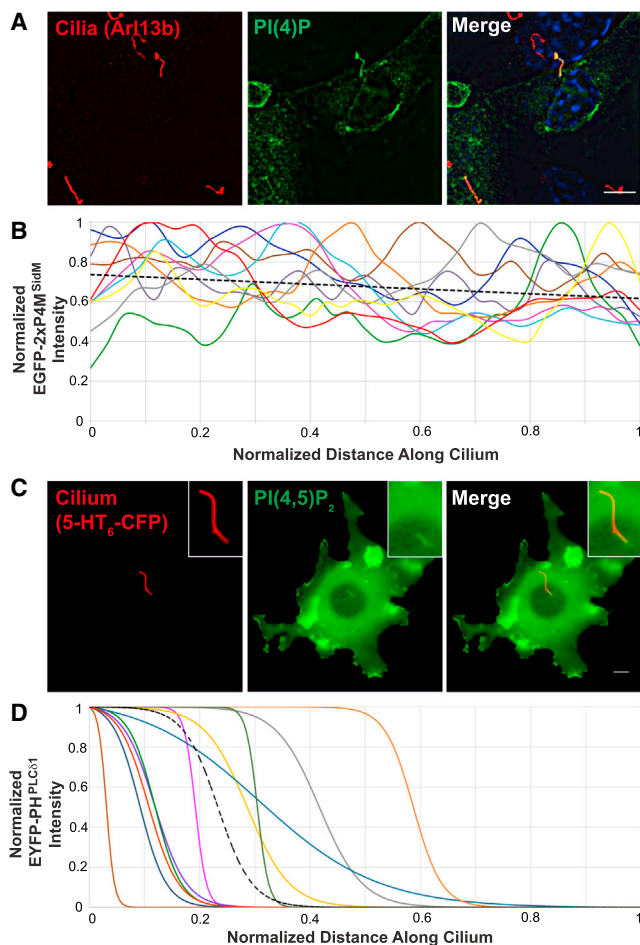
Figure 1. PI(4)P and PI(4,5)P$_2$ Are Present in Distinct Ciliary Compartments

(A) IMCD3 cells transfected with EGFP-2xP4M^{SidM}, a PI(4)P sensor, were stained with antibodies against the ciliary protein Arl13b (red) and EGFP (green). Nuclei were marked by DAPI (blue).

(B) Normalized EGFP-2xP4M^{SidM} intensity for ten IMCD3 cilia was plotted against normalized distance along the cilium. The black dotted line is the linear regression of all cilia.

(C) Cilia of live NIH 3T3 cells were visualized by 5HT$_6$-CFP fluorescence (false-colored red). PH$^{PLC\delta1}$-EYFP, a PI(4,5)P$_2$ sensor, accumulated in the proximal ciliary region (false-colored green). Scale bar, 5 μm.

(D) Normalized EYFP-PH$^{PLC\delta1}$ intensity for 11 NIH 3T3 cilia was plotted against normalized distance along the cilium, and the data were fitted to sigmoidal curves. The black dotted line is the average of all curves.

Scale bars, 5 μm. See also Figure S1.

RESULTS

PI(4)P and PI(4,5)P$_2$ Localize to Distinct Ciliary Compartments

To investigate whether specific phosphoinositides localize to cilia, we expressed specific phosphoinositide-binding domains fused to fluorescent proteins in ciliated cells (Hammond and Balla, 2015). Unlike sensors for PI(3)P, PI(5)P, PI(3,4)P$_2$, PI(3,5)P$_2$, and PIP$_3$, a PI(4)P-specific sensor, EGFP-2xP4M^{SidM} (Hammond et al., 2014), was enriched in cilia (Figure 1A and data not shown). EGFP-2xP4M^{SidM} was present in 74% ± 4% of IMCD3 cilia. Line

scans of ten such cilia reflect the presence of PI(4)P throughout the ciliary membrane (Figure 1B). Antibody staining confirmed the enrichment of PI(4)P within IMCD3 cilia (Figure S1A). Immuno-fluorescence also revealed that sea urchin cilia have abundant PI(4)P, indicating that PI(4)P is a component of the ciliary membrane in evolutionarily distant animals (Figure S1B).

Whereas PI(4)P was present along the length of cilia, a PI(4,5)P$_2$ sensor (EYFP-PH$^{PLC\delta1}$) (Stauffer et al., 1998) localized to the proximal end of NIH 3T3 and IMCD3 cilia (Figure 1C; Figures S1C and S1D). EYFP-PH$^{PLC\delta1}$ fluorescence ceased at a sharp boundary near the ciliary base (Figure 1D). To confirm that EYFP-PH$^{PLC\delta1}$ fluorescence reflected PI(4,5)P$_2$ distribution, we targeted Inp54p, a yeast enzyme that specifically converts PI(4,5)P$_2$ to PI(4)P, to cilia by fusing it to a ciliary GPCR (Serotonin Receptor 6, 5HT$_6$) (Lin et al., 2013; Johnson et al., 2008; Tsujishita et al., 2001; Suh et al., 2006). Coexpression of 5HT$_6$-EYFP-Inp54p with a PI(4,5)P$_2$ sensor (mCerulean3-PH$^{PLC\delta1}$) reduced mCerulean fluorescence at the ciliary base (Figures S1E and S1F). A catalytically inactive version, 5HT$_6$-EYFP-Inp54p(D281A), did not affect mCerulean3-PH$^{PLC\delta1}$ localization (Figures S1E and S1F) (Suh et al., 2006). Conversely, targeting PI(4)P 5-kinase, type Iγ (PIPK) to cilia by fusing it to 5HT$_6$ expanded mCerulean3-PH$^{PLC\delta1}$ localization to the length of the cilium (Figures S1E and S1F) (Suh et al., 2006; Ueno et al., 2011). A catalytically inactive version, 5HT$_6$-EYFP-PIPK(D253A), had no effect on mCerulean3-PH$^{PLC\delta1}$ localization (Figures S1E and S1F) (Ueno et al., 2011). Together, these data indicate that the ciliary membrane contains PI(4)P along its length, and PI(4,5)P$_2$ proximally.

Inpp5e Generates Ciliary PI(4)P and Restricts Ciliary PI(4,5)P$_2$

The transition zone, a region of the ciliary base, participates in protein localization to cilia (Czarnecki and Shah, 2012; Garcia-Gonzalo and Reiter, 2012). We found that Tctn1, a transition zone protein essential for vertebrate Hh signaling (Garcia-Gonzalo et al., 2011; Roberson et al., 2015), is required for the ciliary localization of Inpp5e (Figures 2A and 2B). Because Inpp5e can convert PI(4,5)P$_2$ into PI(4)P, we hypothesized that Inpp5e affects the relative levels of these lipids in the ciliary membrane. To test this hypothesis, we derived mouse embryonic fibroblasts (MEFs) from Inpp5e$^{+/-}$ and Inpp5e$^{-/-}$ embryos (Jacoby et al., 2009). As expected, Inpp5e was present in the cilia of Inpp5e$^{+/-}$ but not Inpp5e$^{-/-}$ MEFs (Figure S2A). Consistent with published data (Jacoby et al., 2009), Inpp5e$^{+/-}$ and Inpp5e$^{-/-}$ MEFs ciliated to equal extents (Figures S2B and S2C). To assess whether Inpp5e affects PI(4)P distribution, we examined the localization of the PI(4)P probe, EGFP-2xP4M^{SidM}, in Inpp5e$^{+/-}$ and Inpp5e$^{-/-}$ MEFs. EGFP-2xP4M^{SidM} localization to cilia was severely reduced in Inpp5e$^{-/-}$ MEFs, further suggesting that EGFP-2xP4M^{SidM} distribution accurately reflects PI(4)P distribution and indicating that Inpp5e is important for generating ciliary PI(4)P (Figures 2C and 2D).

As Inpp5e has the ability to remove the 5-phosphate from PI(4,5)P$_2$, we hypothesized that it regulates ciliary PI(4,5)P$_2$ levels. To test this, we expressed mCerulean3-PH$^{PLC\delta1}$, a PI(4,5)P$_2$ probe, in Inpp5e$^{+/-}$ and Inpp5e$^{-/-}$ MEFs. Similarly to NIH 3T3 and IMCD3 cells, Inpp5e$^{+/-}$ MEFs localized mCerulean-PH$^{PLC\delta1}$ at the proximal cilium (Figures 2E and 2F). In
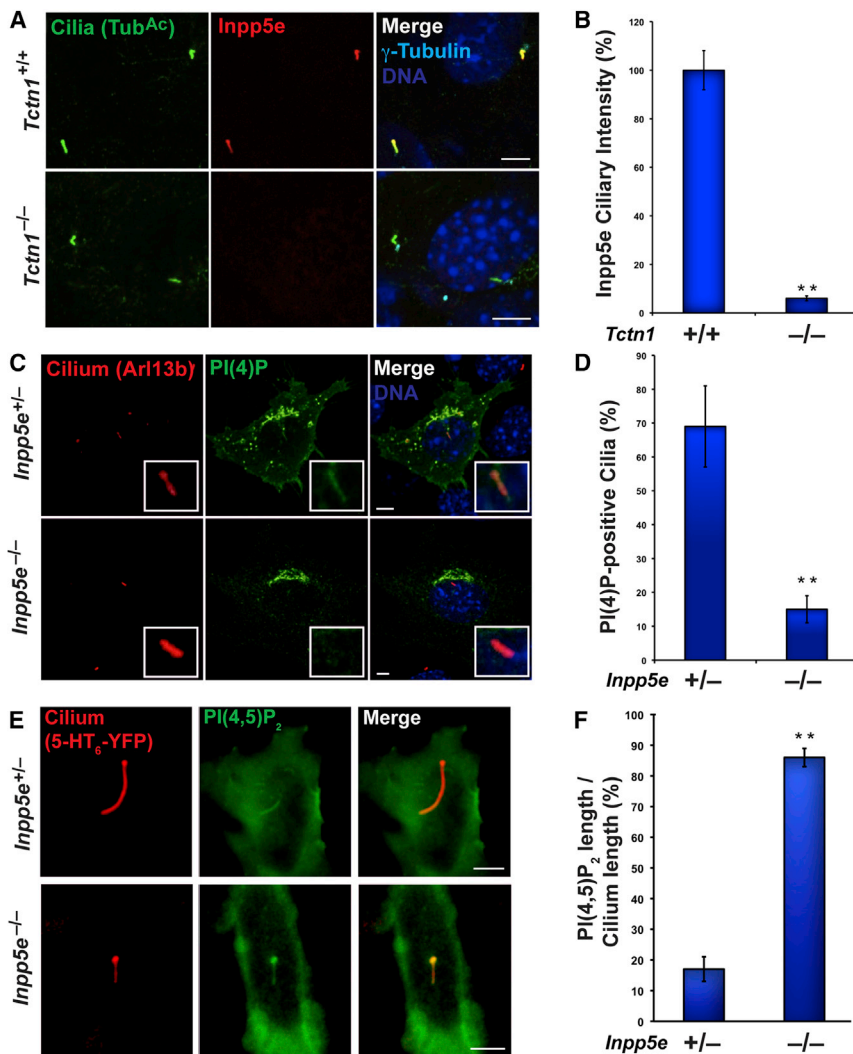
Figure 2. The Ciliopathy Protein Inpp5e Controls Ciliary Phosphoinositide Levels

(A) Wild-type and $Tctn1^{-/-}$ MEFs were stained with antibodies for the ciliary protein acetylated tubulin (Tub^{Ac}, green), Inpp5e (red), and the basal body protein γ-Tubulin (cyan). Nuclei were marked by DAPI (blue).

(B) Quantitation of the amount of Inpp5e fluorescence intensity at cilia of $Tctn1^{-/-}$ MEFs relative to the cilia of wild-type MEFs.

(C) $Inpp5e^{+/-}$ and $Inpp5e^{-/-}$ MEFs expressing the PI(4)P sensor EGFP-2xP4M^{SidM} were stained for Arl13b (red) and EGFP (green). Nuclei were marked by DAPI (blue).

(D) Quantitation of the proportion of $Inpp5e^{+/-}$ and $Inpp5e^{-/-}$ MEF cilia that display ciliary localization of EGFP-2xP4M^{SidM}.

(E) Cilia of live $Inpp5e^{+/-}$ and $Inpp5e^{-/-}$ MEFs were visualized by 5HT$_6$-YFP fluorescence (false-colored red). The PI(4,5)P$_2$ sensor PH^{PLCδ1}-mCerulean3 (false-colored green) localized to a restricted proximal domain of cilia of $Inpp5e^{+/-}$ MEFs but localized throughout cilia of $Inpp5e^{-/-}$ MEFs.

(F) Quantitation of the extent of the ciliary PH^{PLCδ1}-mCerulean3 fluorescence (PI(4,5)P$_2$ length) relative to the extent of 5HT$_6$-YFP fluorescence (cilium length) in $Inpp5e^{+/-}$ and $Inpp5e^{-/-}$ MEFs.

Scale bars, 5 μm. Data are shown as means ± SEM. **$p < 0.01$ in unpaired t tests. See also Figure S2.

Inpp5e Promotes Hedgehog Signaling and Limits Gpr161 Ciliary Localization

Because cilia are required for vertebrate cells to respond to Hh signals, we examined whether Inpp5e is required for Hh signa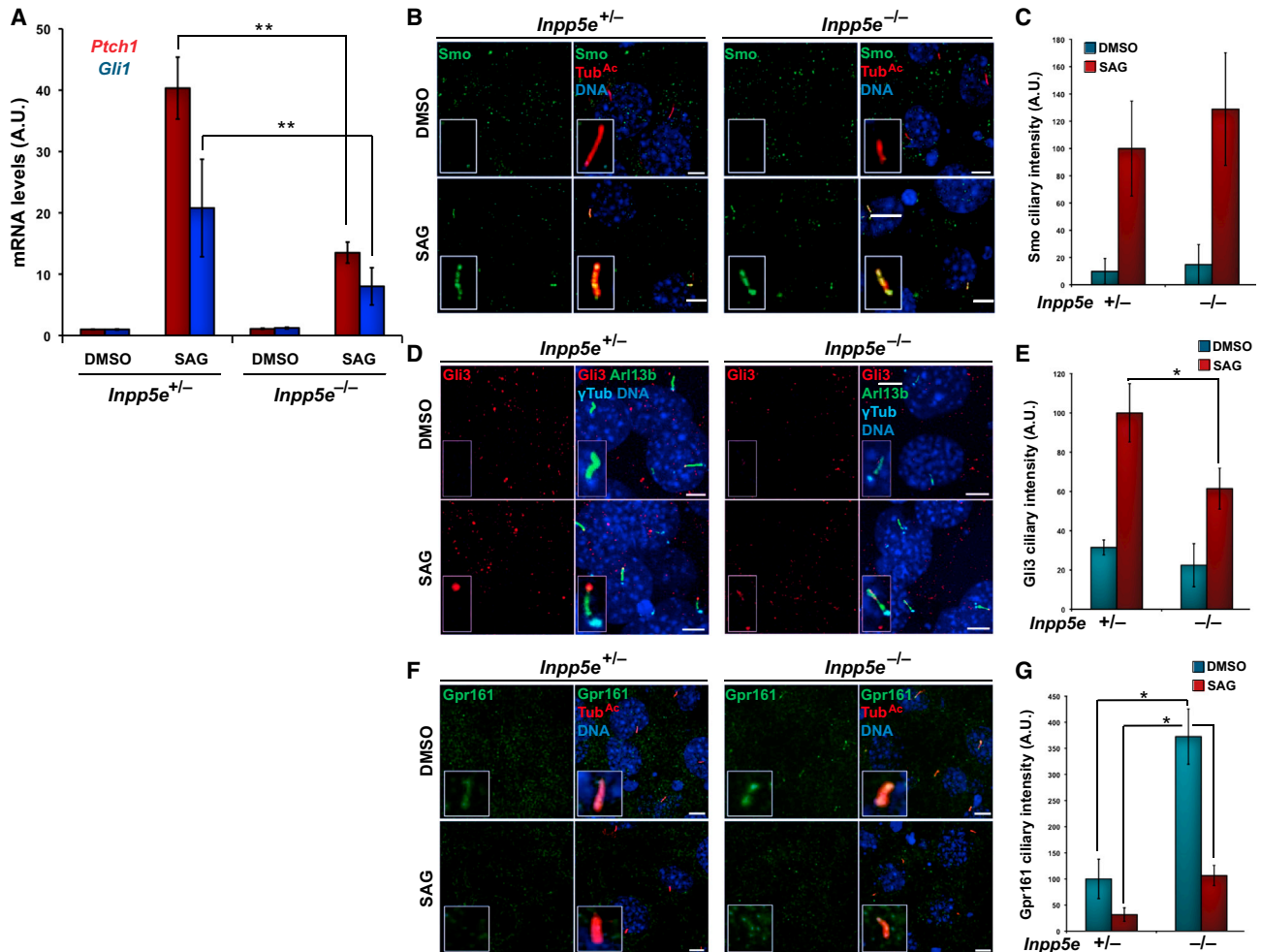l transduction. Stimulating control $Inpp5e^{+/-}$ MEFs with the N-terminal signaling portion of Shh, ShhN, or a pharmacological agonist of Smo, SAG, robustly increased transcription of $Gli1$ and $Ptch1$, two Hh target genes (Figure 3A; Figures S3A–S3C) (Chen et al., 2002). These responses were abrogated in mutant $Inpp5e^{-/-}$ MEFs, revealing a role for Inpp5e in promoting Hh signaling (Figure 3A and Figures S3A–S3C).

To investigate how the Inpp5e-mediated control of ciliary phosphoinositide levels participates in Hh signaling, we examined the subcellular localization of Hh pathway components in control and $Inpp5e^{-/-}$ MEFs. Because Inpp5e is required for cells to respond fully to the Smo agonist SAG (Figure 3A), ciliary phosphoinositides are likely to participate in Hh signaling at the level of, or downstream of, Smo. As expected, Ptch1 localized normally to cilia in $Inpp5e^{-/-}$ MEF (Figure S3D) (Rohatgi et al., 2007). Because CIL-1, a *C. elegans* homolog of Inpp5e, helps control the ciliary localization of PKD-2, another ciliary membrane protein and the ortholog of mammalian Polycystin-2 (Bae et al., 2009), we examined whether Inpp5e also affects the ciliary localization of Polycystin-2. Unlike nematodes, mouse Inpp5e is dispensable for the ciliary localization of Polycystin-2

contrast, $Inpp5e^{-/-}$ MEFs localized mCerulean3-PH^{PLCδ1} along the entire length of the ciliary membrane (Figures 2E and 2F). Thus, Inpp5e limits ciliary PI(4,5)P$_2$ and generates ciliary PI(4)P, consistent with a role in converting PI(4,5)P$_2$ to PI(4)P within cilia.

To test whether the expanded ciliary PI(4,5)P$_2$ in $Inpp5e^{-/-}$ MEFs reflects loss of ciliary PI(4,5)P$_2$ 5-phosphatase activity, we examined whether targeting the yeast PI(4,5)P$_2$ 5-phosphatase Inp54p to cilia lacking Inpp5e restored normal ciliary PI(4,5)P$_2$ levels. 5HT$_6$-EYFP-Inp54p, but not the catalytically inactive 5HT$_6$-EYFP-Inp54p(D281A), restored the ciliary exclusion of mCerulean3-PH^{PLCδ1} in $Inpp5e^{-/-}$ MEFs (Figure S2D). These results further suggest that Inpp5e dephosphorylates ciliary PI(4,5)P$_2$ to restrict it to the proximal cilium.

Because Tctn1 is required to localize Inpp5e to cilia, we hypothesized that, like $Inpp5e^{-/-}$ MEFs, $Tctn1^{-/-}$ MEFs would demonstrate altered ciliary phosphoinositide composition. As with other cell types, the PI(4,5)P$_2$ probe mCerulean3-PH^{PLCδ1} was restricted to the base of $Tctn1^{+/+}$ MEF cilia. In contrast to the wild-type MEFs, but like $Inpp5e^{-/-}$ MEFs, mCerulean3-PH^{PLCδ1} localized along the full length of $Tctn1^{-/-}$ MEF cilia (Figures S2E and S2F).

Figure 3. Inpp5e Promotes Hh Signaling and Limits Gpr161 Localization to Cilia

(A) *Inpp5e*^{+/−} and *Inpp5e*^{−/−} MEFs were treated with SAG or vehicle (DMSO), and expression of Hh target genes *Ptch1* and *Gli1* was measured by qRT-PCR in arbitrary units (a.u.). Error bars represent SDs of six independent experiments. **p < 0.01 in unpaired t tests.

(B) *Inpp5e*^{+/−} and *Inpp5e*^{−/−} MEFs were treated with SAG or vehicle (DMSO) and stained for Smo (green) and Tub[Ac] (red).

(C) Quantitation of Smo ciliary intensity in DMSO or SAG-treated *Inpp5e*^{+/−} and *Inpp5e*^{−/−} MEFs.

(D) *Inpp5e*^{+/−} and *Inpp5e*^{−/−} MEFs were treated with SAG or vehicle (DMSO) and stained for Gli3 (red), Arl13b (green), and γ-Tubulin (γTub, cyan).

(E) Quantitation of Gli3 levels at the ciliary tip in DMSO or SAG-treated *Inpp5e*^{+/−} and *Inpp5e*^{−/−} MEFs.

(F) *Inpp5e*^{+/−} and *Inpp5e*^{−/−} MEFs were treated with SAG or vehicle (DMSO) and stained for Gpr161 (green) and Tub[Ac] (red).

(G) Quantitation of ciliary Gpr161 levels in DMSO or SAG-treated *Inpp5e*^{+/−} and *Inpp5e*^{−/−} MEFs.

Nuclei were marked by DAPI (blue). Error bars represent SDs. *p < 0.05. Scale bars, 5 μm. See also Figure S3.

(Figure S3E). Similarly, Inpp5e was not required either for the exclusion of Smo from cilia in the absence of pathway activation or for its ciliary localization upon stimulation with SAG (Figures 3B and 3C and Figure S3F). In contrast, the SAG-dependent accumulation of Gli3 at the ciliary tip was reduced in *Inpp5e*^{−/−} cells (Figures 3D and 3E and Figure S3G). Therefore, Inpp5e promotes Hh signal transduction at a step subsequent to Smo ciliary localization and prior to Gli3 accumulation at the ciliary tip.

Recently, Gpr161 was identified as a negative regulator of Hh signaling that functions upstream of Gli transcription factor accumulation in cilia (Mukhopadhyay et al., 2013). Remarkably, we observed that ciliary levels of Gpr161 in *Inpp5e*^{−/−} MEFs were greater than in *Inpp5e*^{+/−} MEFs (Figures 3F and 3G). SAG treatment lowered ciliary Gpr161 levels approximately 3-fold in

both cell types relative to unstimulated cells, as a result of which Gpr161 levels remained higher in *Inpp5e*^{−/−} MEFs after SAG treatment (Figure 3G and Figure S3H). Thus, Inpp5e limits ciliary Gpr161 levels but does not prevent the Hh-dependent ciliary exit of Gpr161.

Inpp5e Limits the Ciliary Localization of Tulp3 and IFT-A

Because the ciliary localization of Gpr161 requires Tulp3, a protein that binds PI(4,5)P$_2$ and that, like Gpr161, restrains vertebrate Hh signaling (Mukhopadhyay et al., 2010, 2013), we examined whether Inpp5e affects Tulp3 localization. Consistent with a previous report (Norman et al., 2009), Tulp3 was only occasionally observed within control cilia (Figures 4A and 4B). In contrast, Tulp3 robustly accumulated along the full length of
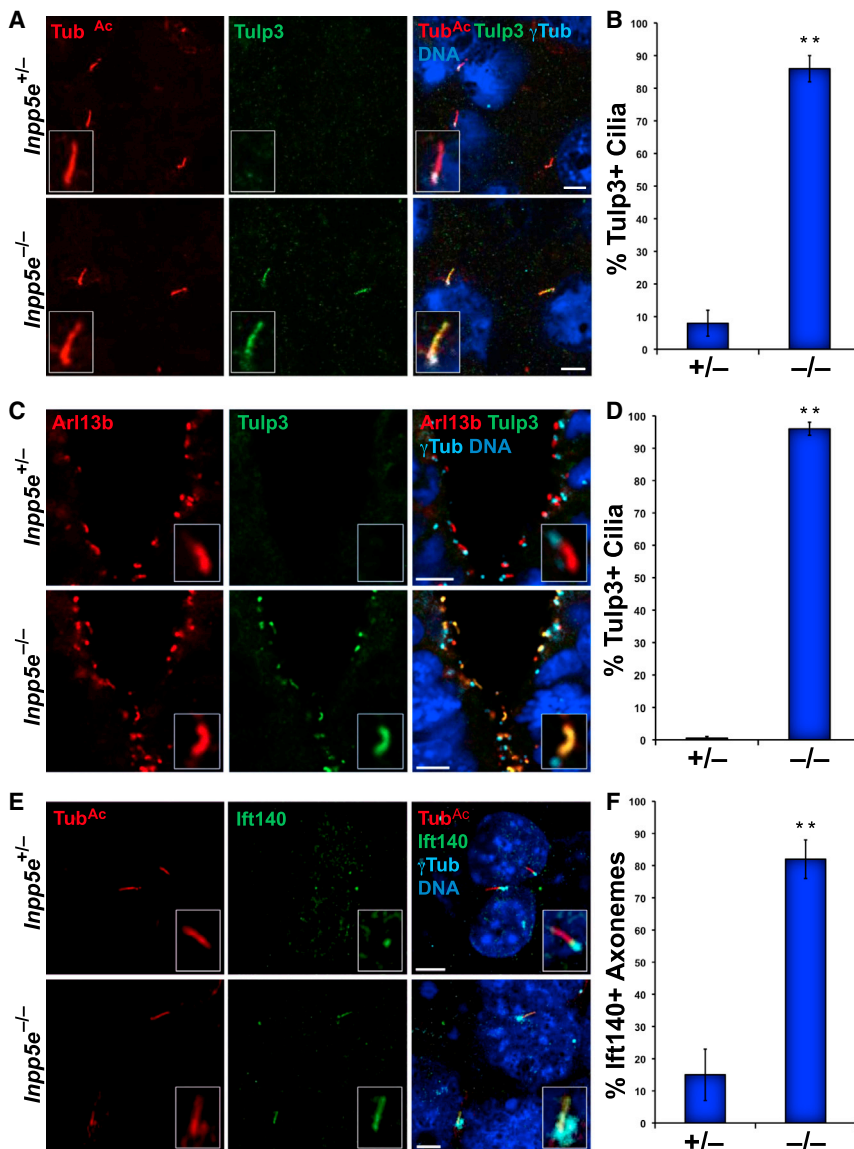
Figure 4. Inpp5e Limits the Ciliary Levels of Tulp3 and IFT-A

(A) *Inpp5e*$^{+/-}$ and *Inpp5e*$^{-/-}$ MEFs were stained for Tub^{Ac} (red), Tulp3 (green), and γTub (cyan). Nuclei were marked by DAPI in all panels (blue).

(B) Quantitation of the percentage of *Inpp5e*$^{+/-}$ and *Inpp5e*$^{-/-}$ MEF cilia containing Tulp3 along their length.

(C) Staining of E9.5 *Inpp5e*$^{+/-}$ and *Inpp5e*$^{-/-}$ neural tubes for Arl13b (red), Tulp3 (green), and γTub (cyan).

(D) Quantitation of the percentage of Tulp3-containing cilia in *Inpp5e*$^{+/-}$ and *Inpp5e*$^{-/-}$ neural tubes.

(E) *Inpp5e*$^{+/-}$ and *Inpp5e*$^{-/-}$ MEFs were stained for Tub^{Ac} (red), Ift140 (green), and γTub (cyan).

(F) Quantitation of the percentage of *Inpp5e*$^{+/-}$ and *Inpp5e*$^{-/-}$ MEF cilia containing Ift140 beyond the basal body.

Data are means ± SEM. **p < 0.01 in unpaired t tests. Scale bars, 5 μm. See also Figure S4.

Tulp3, and Gpr161. Because these proteins interact with each other, we hypothesized that the phosphoinositide levels controlled by Inpp5e limit their localization to cilia.

Since *Tctn1*$^{-/-}$ MEF cilia, like those of *Inpp5e*$^{-/-}$ MEFs, lack Inpp5e and accumulate PI(4,5)P$_2$, we tested whether they also accumulate Tulp3 and Gpr161. Ciliary levels of Tulp3 in *Tctn1*$^{-/-}$ MEFs were not increased (Figure S4D), and ciliary levels of Gpr161 were decreased in *Tctn1*$^{-/-}$ MEFs (Figure S4E). Given that many other membrane-associated proteins, such as Polycystin-2 and Smo, fail to localize to cilia in *Tctn1*$^{-/-}$ MEFs but localize normally to the cilia of *Inpp5e*$^{-/-}$ MEFs (Garcia-Gonzalo et al., 2011 and this work), we conclude that the disruption of the ciliary gate at the transition zone caused by loss of Tctn1 leads to a more pervasive defect in localizing ciliary membrane-associated proteins than does absence of ciliary Inpp5e.
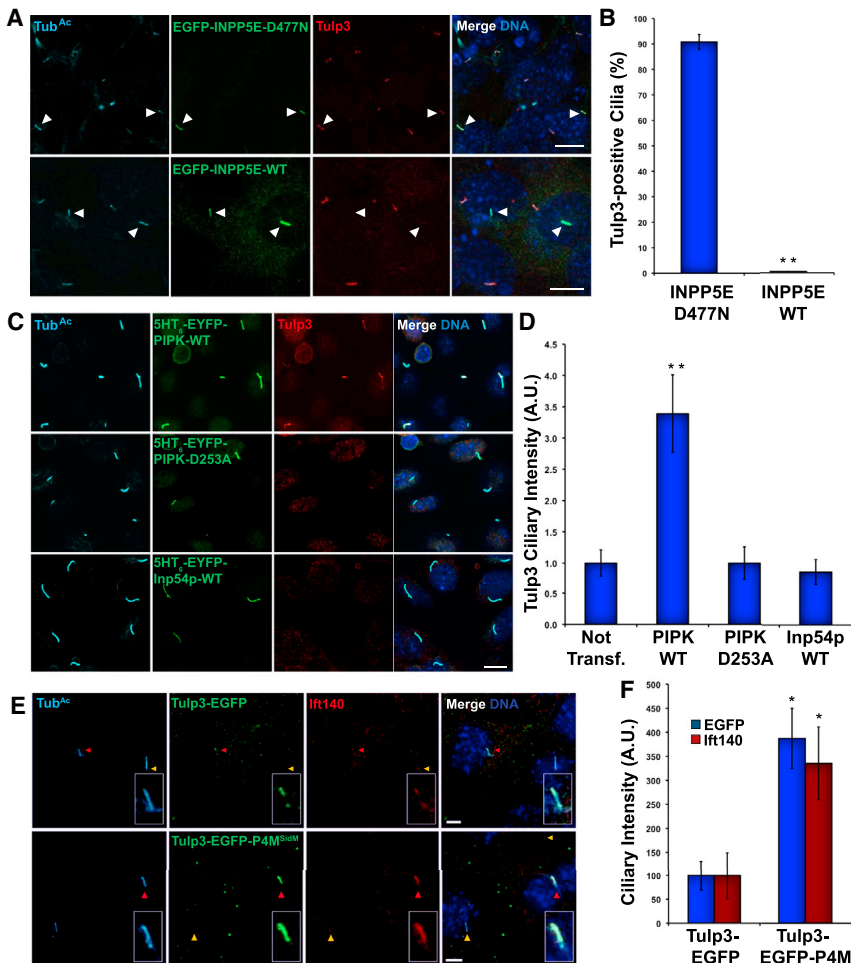
Inpp5e$^{-/-}$ MEF cilia (Figures 4A and 4B). Tulp3 was also present at abnormally high levels in the primary cilia of *Inpp5e*$^{-/-}$ E9.5 neural tubes and other tissues (Figures 4C and 4D and data not shown). Immunoblot analysis revealed that Tulp3 levels are equivalent in *Inpp5e*$^{+/-}$ and *Inpp5e*$^{-/-}$ MEFs (Figure S4A), suggesting that ciliary phosphoinositides affect Tulp3 localization to cilia but not its stability.

Tulp3 interacts with the IFT-A complex, and IFT-A components such as Ift139 (also called Thm1 or Ttc21b) restrain vertebrate Hh signaling, similar to Tulp3 and Gpr161 (Qin et al., 2011; Tran et al., 2008; Liem et al., 2012). Therefore, we investigated whether Inpp5e also restricts the ciliary localization of IFT-A components. Like Tulp3, IFT-A components Ift139 and Ift140 overaccumulated in the cilia of *Inpp5e*$^{-/-}$ MEFs (Figures 4E and 4F and Figure S4B). In contrast, loss of Inpp5e did not affect the ciliary levels of IFT-B component Ift88 (Figure S4C). Thus, in addition to promoting Hh signaling, Inpp5e limits the ciliary localization of the Hh-signaling negative regulators Ift139, Ift140,

Inpp5e Limits Ciliary Tulp3 and IFT-A Levels by Restricting Ciliary PI(4,5)P$_2$

To determine whether the ciliary buildup of Tulp3 in *Inpp5e*$^{-/-}$ cells was due to the elevated ciliary PI(4,5)P$_2$ levels, we tested whether expression of wild-type or catalytically dead Inpp5e affected ciliary Tulp3 levels. Expression of EGFP-INPP5E-WT in *Inpp5e*$^{-/-}$ cilia removed Tulp3 from cilia, whereas catalytically inactive EGFP-INPP5E-D477N had no effect, consistent with a phosphatase-dependent role for Inpp5e in controlling ciliary Tulp3 levels (Figures 5A and 5B).

To assess whether PI(4,5)P$_2$ is sufficient to cause Tulp3 to accumulate in cilia, we targeted a PI(4)P 5-kinase (5HT$_6$-EYFP-PIPK) to the cilia of wild-type IMCD3 cells. As shown previously, 5HT$_6$-EYFP-PIPK increases ciliary PI(4,5)P$_2$ levels (Figures S1E

P4M^{SidM}, like Tulp3 in cilia with elevated PI(4,5)P$_2$ levels, robustly localized to cilia (Figures 5E and 5F). These results suggest that persistent interaction with phosphoinositides of the ciliary membrane is sufficient to increase the ciliary localization of Tulp3 and that increased ciliary PI(4,5)P$_2$ levels are sufficient to increase ciliary localization of Tulp3.

To assess whether altered ciliary Tulp3-phosphoinositide interactions are sufficient to affect the localization of Tulp3-interacting proteins, we examined whether Tulp3-EGFP-P4M^{SidM} affected the ciliary localization of Ift140. Expression of Tulp3-EGFP-P4M^{SidM} caused Ift140 to accumulate in cilia (Figures 5E and 5F), similar to the accumulation of Ift140 in *Inpp5e*$^{-/-}$ cells, whereas expression of Tulp3-EGFP had no effect on ciliary Ift140. These results are consistent with differential Tulp3 interaction with PI(4,5)P$_2$ in the membrane of the ciliary base and PI(4)P in the more distal ciliary membrane being critical to limit the ciliary localization of both Tulp3 and its interacting protein, Ift140.

Inhibition of Tulp3 or Gpr161 Increases Hh Signaling in *Inpp5e*$^{-/-}$ MEFs

We hypothesized that the Hh signaling defects caused by loss of Inpp5e were due to the PI(4,5)P$_2$-dependent increase in ciliary Tulp3 and its associated proteins, including Gpr161. We reduced Tulp3 and Gpr161 levels in *Inpp5e*$^{-/-}$ MEFs using small interfering RNA (siRNA)-mediated knockdown (Figures S6A–S6C). Reducing Tulp3 reduced the ciliary levels of Gpr161, consistent with a role for Tulp3 in delivering Gpr161 to the cilium (Figures S6A and S6C). In contrast, reducing Gpr161 had no

and S1F). In addition to increasing ciliary PI(4,5)P$_2$ levels, 5HT$_6$-EYFP-PIPK increased ciliary Tulp3 levels (Figures 5C and 5D). In contrast, the inactive mutant 5HT$_6$-EYFP-PIPK-D253A or 5HT$_6$-EYFP-Inp54p had no such effect (Figures 5C and 5D).

Because Tulp3 is required for the ciliary delivery of Gpr161, we tested whether increasing ciliary PI(4,5)P$_2$ levels also increased ciliary Gpr161 localization. Expression of 5HT$_6$-EYFP-PIPK caused a modest but significant increase in ciliary Gpr161 levels as compared to expression of 5HT$_6$-EYFP-PIPK-D253A (Figures S5A and S5B). Because increasing ciliary PI(4,5)P$_2$ levels—either by removing Inpp5e or by increasing ciliary PI(4)P 5-kinase activity—increased ciliary levels of Tulp3 and Gpr161, we conclude that maintaining low ciliary PI(4,5)P$_2$ levels is critical for restraining ciliary Tulp3 and Gpr161 localization.
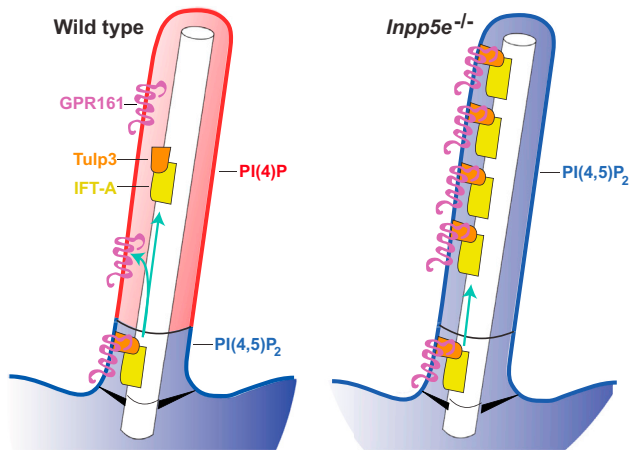
Tulp3 binds PI(4,5)P$_2$ but not PI(4)P (Mukhopadhyay et al., 2010). We hypothesized that this phosphoinositide binding specificity accounted for the limited localization of Tulp3 to cilia of wild-type cells and the increased localization of Tulp3 to cilia with increased PI(4,5)P$_2$ levels. To test this hypothesis, we generated a Tulp3 with altered phosphoinositide binding specificity by fusing Tulp3-EGFP to P4M^{SidM}, a PI(4)P-binding domain of a Legionella protein (Hammond et al., 2014). Whereas, like endogenous Tulp3, Tulp3-EGFP weakly localized to cilia, Tulp3-EGFP-

Figure 6. Model of the Role of Ciliary Phosphoinositides in Hh Signaling

Inpp5e restricts PI(4,5)P$_2$ levels in the ciliary membrane. The ability of Tulp3 to interact with PI(4,5)P$_2$ but not PI(4)P is critical for limiting its accumulation and that of its interactors IFT-A and Gpr161 within the cilium. In the absence of Inpp5e, ciliary PI(4,5)P$_2$ levels increase, increasing the amount of negative regulators of Hh signaling, Tulp3, IFT-A, and Gpr161, within the cilium and restricting the ability of the cilium to transduce Hh signals.

See also Figure S6.

effect on the ciliary levels of Tulp3, indicating that there is no reciprocal requirement (Figures S6A and S6C).

In addition to decreasing ciliary Gpr161 levels, depletion of Tulp3 increased SAG-activated Hh signaling in *Inpp5e*$^{-/-}$ MEFs to a level indistinguishable from that of control cells (Figure S6D). Depletion of Gpr161 in *Inpp5e*$^{-/-}$ MEFs led to a more modest but still significant increase in SAG-activated Hh signaling (Figures S6D and S6E). We conclude, therefore, that limiting ciliary PI(4,5)P$_2$ levels is critical for restricting the ciliary localization of Tulp3 and other negative regulators of Hh signaling (Figure 6). Defects in maintaining the normal distribution of ciliary phosphoinositides alters ciliary trafficking of Tulp3, IFT-A, and Gpr161, disrupting ciliary Hh signaling.

DISCUSSION

Phosphoinositides help confer identity to organelles. For example, endosome and Golgi membranes possess PI(3)P and PI(4)P, respectively (Di Paolo and De Camilli, 2006; Roth, 2004), whereas the plasma membrane possesses both PI(4)P and PI(4,5)P$_2$ (Hammond et al., 2012, 2014). Physical separation of these membrane-bound organelles makes their distinct lipid compositions possible. In contrast to most organelles, the cilium is not membrane-bounded. Despite this difference, we found a sharp boundary at the ciliary base that separates the ciliary membrane into a distal PI(4)P-containing domain and a proximal PI(4,5)P$_2$-containing domain.

Creating this phosphoinositide boundary depends on the Tctn1 complex of the transition zone to confine the Inpp5e phosphatase within the cilium. We previously showed that Tctn1 and other components of the transition zone MKS complex are critical for localizing the small GTPase Arl13b to the cilium (Garcia-Gonzalo et al., 2011). Arl13b is itself critical for the ciliary

localization of Inpp5e (Humbert et al., 2012). Thus, it is likely that Tctn1 and the transition zone MKS complex localize Inpp5e to cilia through their effects on Arl13b.

In the absence of Inpp5e, ciliary levels of PI(4)P decrease and levels of PI(4,5)P$_2$ increase, suggesting that Inpp5e is critical for generating the observed distribution of ciliary phosphoinositides. It will be interesting to determine whether Inpp5e shares this function with other ciliary phosphoinositide phosphatases, such as Ocrl or Inpp5b (Luo et al., 2012, 2013).

Perturbing the ciliary levels of ciliary PI(4)P and PI(4,5)P$_2$, either by removing Inpp5e or by targeting the phosphoinositide 5-kinase PIPK to cilia, is sufficient to increase the ciliary localization of Tulp3. Because Tulp3 interacts with PI(4,5)P$_2$ but not PI(4)P (Mukhopadhyay et al., 2010), it is an excellent candidate for distinguishing between these two domains within the cilium. Tulp3 binds to the IFT-A complex to deliver GPCRs such as Gpr161 to cilia (Mukhopadhyay et al., 2010, 2013). Consistent with a critical role for Tulp3-mediated sensing of phosphoinositides in this process, disruption of the ciliary phosphoinositide distribution not only increases ciliary Tulp3 but also increases the ciliary levels of IFT-A components and Gpr161. Although Tulp3 is one key interpreter of ciliary phosphoinositides, it may not be the sole one. Other Tubby family proteins may share this role. Mutation of either Tubby or Tulp1 causes retinal degeneration, a phenotype commonly observed in ciliopathies (Mukhopadhyay and Jackson, 2011). By analogy to our findings with Tulp3 and Gpr161, it is possible that photoreceptor phosphoinositides are read out by Tubby and Tulp1 to control the delivery of Rhodopsin to the outer segment, defects that cause photoreceptor loss.

Tulp3, IFT-A components such as Ift139, and Gpr161 are all negative regulators of ciliary Hh signaling (Mukhopadhyay et al., 2013; Norman et al., 2009; Patterson et al., 2009; Cameron et al., 2009; Qin et al., 2011; Tran et al., 2008; Liem et al., 2012). In addition to limiting ciliary PI(4,5)P$_2$ levels, Inpp5e limits the ciliary localization of these negative regulators and is required for normal Hh signal transduction. Reducing Tulp3 levels in cilia using an siRNA restores Hh signaling in MEFs lacking Inpp5e, suggesting that overaccumulation of Tulp3 in cilia is a key factor in the observed signaling defects. The effect of the *Tulp3* siRNA on Hh signaling is consistent with the effect of loss-of-function mutations in *Tulp3* on developmental Hh signaling, suggesting that the siRNA effect is on target, but it will be of interest to confirm this epistasis using genetic tools (Norman et al., 2009; Patterson et al., 2009; Cameron et al., 2009). Reducing Gpr161 levels also increased Hh signaling in *Inpp5e*$^{-/-}$ MEFs, suggesting that it is also sufficient to limit normal Hh signaling. The more modest effect of reducing Gpr161 levels, reflected by the fact that the fold induction of *Ptch1* by SAG was unaffected by Gpr161 depletion, raises the possibility that overaccumulation of Tulp3 in cilia also causes the ciliary accumulation of additional negative regulators of Hh signaling. Our finding that reducing Tulp3 or Gpr161 levels increases Hh response even in the presence of increased ciliary PI(4,5)P$_2$ indicates that control of these two protein levels is a critical role for ciliary phosphoinositides in Hh signaling.

In mammalian cells, Tulp3 interprets ciliary phosphoinositides to control the localization of interactors such as IFT-A components and Gpr161. Increasing the ciliary levels of PI(4,5)P$_2$ (by loss of Inpp5e or by expressing a ciliary phosphoinositide

5-kinase) or fusing Tulp3 with a PI(4)P-binding domain increases the ciliary localization of Tulp3 and IFT-A components. Therefore, restricting ciliary PI(4,5)P$_2$ levels is critical to limiting the ciliary localization of Tulp3 and its interactors. Thus, the interplay between proteins and lipids helps generate the specialized subcellular environment present in the primary cilium and is critical for its ability to transduce signals.

In most *Drosophila* cells, the Hh pathway functions independently of cilia, yet PI(4)P is required for *Drosophila* Hh signaling (Yavari et al., 2010). Although the cellular contexts may be different, a membrane domain high in PI(4)P and low in PI(4,5)P$_2$ may represent a fundamental requirement for the cilium-dependent and cilium-independent transduction of Hh signals. We did not successfully observe rescue of Hh signaling by overexpressing Inpp5e in *Inpp5e*$^{-/-}$ MEFs (data not shown). This is likely due to inefficient transfection of *Inpp5e*$^{-/-}$ MEFs, but it also raises the possibility that overexpressed Inpp5e inhibits other aspects of ciliary function, perhaps by altering phosphoinositide pools recognized by FAPP2, a Golgi protein involved in ciliogenesis, or the BBSome (Vieira et al., 2006; Jin et al., 2010).

Just as PI(4)P may have functions in Hh signaling that are independent of cilia, it is possible that PI(4,5)P$_2$ may have functions in cilia that predate the origin of Hh signaling. Although the ciliary phosphoinositide composition of unicellular organisms has not yet been determined, the wide phylogenetic distribution of Tubby family proteins hints at a broad and evolutionarily ancient role for PI(4,5)P$_2$ in ciliary biology. For example, Tubby family members are present in many ciliated organisms, such as *Chlamydomonas*, *Tetrahymena*, and *Paramecium*. Determining whether Tubby proteins interpret ciliary phosphoinositides to regulate ciliary protein delivery in these organisms will help reveal the evolutionary origins of the role of phosphoinositides in ciliary function.

We have shown that the ciliary membrane has a distinct phosphoinositide composition that is critical for regulating ciliary protein trafficking and, thus, Hh signal transduction. Importantly, this role does not exclude additional roles for ciliary phosphoinositides, including as cofactors for ciliary protein function, determinants of ciliary membrane viscosity, or contributors to membrane surface charge or ion-binding capacity. The specialized compositions of ciliary proteins and lipids depend on each other and are essential for generating the specialized environment that makes the cilium a unique signaling organelle.

EXPERIMENTAL PROCEDURES

Animal Models and Cell Lines

Inpp5e$^{-/-}$ mice have been described previously, as have *Tctn1*$^{-/-}$ mice and MEFs (Jacoby et al., 2009; Garcia-Gonzalo et al., 2011; Reiter and Skarnes, 2006). We derived MEFs from littermate E19.5 *Inpp5e*$^{+/-}$ and *Inpp5e*$^{-/-}$ embryonic tails. Briefly, tails were dissected, rinsed in Dulbecco's PBS containing penicillin and streptomycin (PenStrep), digested for 10 min in 0.05% Trypsin-EDTA, disaggregated by pipetting, and plated on DMEM medium supplemented with 20% FBS and PenStrep. These primary MEFs were maintained in DMEM, 15% FBS, and PenStrep and immortalized by infection with a lentivirus expressing SV40 large T antigen. All MEF experiments in this study were performed using immortalized MEFs grown in DMEM and 10% FBS. All mouse protocols were approved by the Institutional Animal Care and Use Committee (IACUC) at the University of California, San Francisco.

For cilia isolation from sea urchin embryos, eggs and sperm from adult *Strongylocentrotus purpuratus* (Kerckhoff Marine Lab) were collected, com-

bined, and cultured for 2 days in natural seawater at ~10,000 embryos/ml at 12°C with constant stirring. Midgastrula embryos were collected, concentrated by centrifugation, and washed three times with natural seawater. Pelleted embryos were resuspended in natural seawater + 0.5M NaCl to amputate cilia. Deciliated embryos were removed from the sample by centrifugation at 400 × *g* for 5 min. Cilia were then pelleted from the supernatant by centrifugation at 10,000 × *g*, 20 min, 4°C.

Immunofluorescence

Antibodies used in this study were: goat anti-γ-Tubulin (Santa Cruz, sc-7396), chicken anti-EGFP (Aves Labs, GFP-1020), mouse anti-acetylated tubulin (Sigma, 6-11B-1), anti-Arl13b (NeuroMab, 75-287), anti-Gli3 (Gli3N-6F5) (Wen et al., 2010), anti-PI4P (Echelon Bioscience, Z-P004), rabbit anti-Inpp5e (Jacoby et al., 2009), anti-Arl13b (Caspary et al., 2007), anti-Smoothened (Abcam, ab38686), anti-Patched1 (Rohatgi et al., 2007), anti-Tulp3 (Norman et al., 2009), anti-Ift140 (Proteintech, 17460-1-AP), and anti-Gpr161 (Proteintech, 13398-1-AP and Mukhopadhyay et al., 2013). For immunostaining of MEFs, cells were grown on coverslips and fixed with 4% PFA in PBS for 5–10 min at room temperature (RT) followed by 3 min at −20°C in cold methanol. PFA fixation was omitted when staining for Ift140. PI4P antibody was used according to the manufacturer's instructions. For Tulp3 staining, cells were fixed for 10 min at 4°C in acetone. After fixation, cells were blocked in PBS containing 0.1% Triton X-100 and 2% donkey serum. For chicken EGFP staining, cells were also blocked in BlokHen-II reagent (Aves Labs) diluted in PBS. After blocking, cells were incubated in block containing primary antibodies for 1 hr at 37°C, 3 hr at RT, or overnight at 4°C. Coverslips were then rinsed twice in PBS, incubated with secondary antibodies and Hoechst 33342 or DAPI (30 min at 37°C or 1 hr at RT), rinsed twice in milliQ water, and mounted in gelvatol. For mouse embryo analyses, we fixed dissected embryos for 1–2 hr in 4% PFA in PBS, washed three times in PBS, and sunk overnight in 30% sucrose. Embryos were then equilibrated and frozen in OCT compound (Sakura) using a dry ice-ethanol bath. For staining, cryosections were thawed and washed three times in PBST (PBS with 0.1% Triton), encircled with an ImmEdge hydrophobic pen, and blocked and stained with antibodies as above. All imaging was performed using a Leica TCS SPE confocal microscope except for Figure 1A, where a Nikon N-SIM Ti-E microscope was used.

Live-Cell Imaging

NIH 3T3, mIMCD3, and MEFs were cultured in DMEM (GIBCO) supplemented with 10% FBS. For all transient transfections, cells were transfected with the respective DNA constructs by plating them directly in a transfection solution containing DNA plasmid and Xtremegene 9 (Roche). Cells were plated on poly(D-lysine)-coated borosilicate glass Lab-Tek 8-well chambers (Thermo Scientific). Ciliogenesis was induced by serum starvation for 24 hr. Live-cell imaging was mostly performed using an IX-71 (Olympus) microscope with a 40× oil objective (Olympus) (with additional 1.6× optical zoom) and a CoolSNAP HQ charge-coupled device camera (Photometrics). Micrographs were taken using MetaMorph 7.5 imaging software (Molecular Devices).

DNA Constructs

To construct the 5HT$_6$-EYFP expression plasmid, we amplified DNA encoding 5HT$_6$ flanked by 5' and 3' AgeI cleavage sites by PCR from 5HT$_6$-EGFP (Berbari et al., 2008) and subcloned it into pEYFP-C1 (Clontech). To construct the 5HT$_6$-EYFP-PIPK, 5HT$_6$-EYFP-PIPK(D253A), 5HT$_6$-EYFP-Inp54p, and 5HT$_6$-EYFP-Inp54p(D281A) expression plasmids, we digested DNAs encoding the wild-type or mutant forms of PIPK or Inp54p from CFP-FKBP-PIPK or CFP-FKBP-Inp54p (Suh et al., 2006) with 5' EcoRI and 3' BamHI cleavage sites and subcloned them into the 5HT$_6$-EYFP expression plasmid. To generate pEGFP-Tulp3-P4MSidM, we amplified the Tulp3 ORF flanked by 5' BglII and 3' XhoI sites by PCR from pGLAP3-Tulp3 (Mukhopadhyay et al., 2010) and subcloned it into pEGFP-2xP4MSidM (Hammond et al., 2014). We created pEGFP-INPP5E-D477N from pEGFP-INPP5E-WT (Jacoby et al., 2009) using site-directed mutagenesis (QuikChange, Agilent).

Hh Signal Transduction Assay

MEFs were plated on 12-well plates in full medium and allowed to reach confluency. The medium was replaced by OptiMEM containing either vehicle, 200 nM SAG (Cayman Chemicals), or 1 μg/ml mouse recombinant ShhN-C25II (R&D

Systems). Cells were then incubated for 24 hr and RNA extracted (QIAGEN RNeasy kit). For each sample, 1 μg RNA was used to make cDNA (Invitrogen Superscript III reverse transcriptase kit). The cDNAs were then analyzed by qPCR using Express SYBR GreenER Supermix with premixed ROX (Invitrogen) and primers for *Gli1*, *Ptch1*, and *β-actin* (Santos and Reiter, 2014). For siRNA transfections, 400,000 cells/well were reverse-transfected in 12-well plates using Lipofectamine-RNAiMAX (Invitrogen). Transfection media were replaced 24 hr later with full medium and cells were incubated for an additional 24 hr, when Hh agonist-containing media were added, as described above.

Quantitations and Statistical Tests

MetaMorph image analysis software was used to quantitate the relative extension of the PI(4,5)P$_2$ ciliary compartment. Only cilia that lied flat on the cell surface were analyzed to ensure accuracy. Cilia length was measured by tracing a line along the ciliary marker signal. PH-PLCδ signal length was measured analogously and expressed as percentage relative to cilia length. For phosphoinositide sensor signal line scans, a line was traced along the length of each cilium (Sensor$_{cilium}$), and a second identical line (Sensor$_{background}$) was traced in close proximity to the first line within the cell area. Normalized values of (Sensor$_{cilium}$ − Sensor$_{background}$) were plotted against relative distance along the cilium and fitted to sigmoid curves if appropriate.

Quantitation of ciliary signal intensities was carried out using ImageJ software. Each experiment was performed at least three times. Z stacks of seven fields of cells were acquired from each condition using a 63× objective and 1.5× digital zoom in a Leica TCS SPE confocal microscope. For each field, a maximal z projection was created and cilia were identified using Arl13b or Tub^{Ac} and γ-Tub as markers. Each cilium (or its tip for Gli3) was outlined with the polygon tool, and the mean intensity of the desired channel inside the area was measured in an 8-bit scale (0–255). These values were then background-subtracted and averaged for each field, which typically contained ten or more cilia. Means and SEMs were then calculated for each condition, and significance was assessed using unpaired, one-tailed homoscedastic Student's t tests. In cases where cilia clearly fell into positive and negative categories, cilia were counted visually and data treated as above. For Tulp3 and Ift140 in MEFs, cilia were only counted as positive if the marker was present inside the cilium, not just at the transition zone.

For Hh assays, qPCR data were analyzed using the ΔΔCt method. Means and SEMs of at least three independent experiments, each run in triplicate, were calculated and plotted, and significance was assessed by Student's t tests as above.

SUPPLEMENTAL INFORMATION

Supplemental Information includes six figures and can be found with this article online at http://dx.doi.org/10.1016/j.devcel.2015.08.001.

AUTHOR CONTRIBUTIONS

F.R.G., S.C.P., T.I., and J.F.R. devised all the experiments, most of which were executed by F.R.G. and S.C.P. Western blots and SIM imaging were performed by E.C.R. and G.G., respectively. Sea urchin flagella and *Inpp5e* mutant mice were generated by M.A and S.S., respectively. F.R.G., S.C.P., T.I., and J.F.R. wrote the manuscript. T.I. and J.F.R. supervised the work.

REFERENCES

Andrews, D., and Nelson, D.L. (1979). Biochemical studies of the excitable membrane of Paramecium tetraurelia. II. Phospholipids of ciliary and other membranes. Biochim. Biophys. Acta *550*, 174–187.

Bae, Y.K., Kim, E., L'hernault, S.W., and Barr, M.M. (2009). The CIL-1 PI 5-phosphatase localizes TRP Polycystins to cilia and activates sperm in C. elegans. Curr. Biol. *19*, 1599–1607.

Berbari, N.F., Johnson, A.D., Lewis, J.S., Askwith, C.C., and Mykytyn, K. (2008). Identification of ciliary localization sequences within the third intracellular loop of G protein-coupled receptors. Mol. Biol. Cell *19*, 1540–1547.

Bielas, S.L., Silhavy, J.L., Brancati, F., Kisseleva, M.V., Al-Gazali, L., Sztriha, L., Bayoumi, R.A., Zaki, M.S., Abdel-Aleem, A., Rosti, R.O., et al. (2009). Mutations in INPP5E, encoding inositol polyphosphate-5-phosphatase E, link phosphatidyl inositol signaling to the ciliopathies. Nat. Genet. *41*, 1032–1036.

Bloodgood, R.A., Woodward, M.P., and Young, W.W., Jr. (1985). Unusual distribution of a glycolipid antigen in the flagella of Chlamydomonas. Protoplasma *185*, 123–130.

Cameron, D.A., Pennimpede, T., and Petkovich, M. (2009). Tulp3 is a critical repressor of mouse hedgehog signaling. Dev. Dyn. *238*, 1140–1149.

Caspary, T., Larkins, C.E., and Anderson, K.V. (2007). The graded response to Sonic Hedgehog depends on cilia architecture. Dev. Cell *12*, 767–778.

Chen, J.K., Taipale, J., Young, K.E., Maiti, T., and Beachy, P.A. (2002). Small molecule modulation of Smoothened activity. Proc. Natl. Acad. Sci. USA *99*, 14071–14076.

Czarnecki, P.G., and Shah, J.V. (2012). The ciliary transition zone: from morphology and molecules to medicine. Trends Cell Biol. *22*, 201–210.

Di Paolo, G., and De Camilli, P. (2006). Phosphoinositides in cell regulation and membrane dynamics. Nature *443*, 651–657.

Forte, M., Satow, Y., Nelson, D., and Kung, C. (1981). Mutational alteration of membrane phospholipid composition and voltage-sensitive ion channel function in paramecium. Proc. Natl. Acad. Sci. USA *78*, 7195–7199.

Garcia-Gonzalo, F.R., and Reiter, J.F. (2012). Scoring a backstage pass: mechanisms of ciliogenesis and ciliary access. J. Cell Biol. *197*, 697–709.

Garcia-Gonzalo, F.R., Corbit, K.C., Sirerol-Piquer, M.S., Ramaswami, G., Otto, E.A., Noriega, T.R., Seol, A.D., Robinson, J.F., Bennett, C.L., Josifova, D.J., et al. (2011). A transition zone complex regulates mammalian ciliogenesis and ciliary membrane composition. Nat. Genet. *43*, 776–784.

Gealt, M.A., Adler, J.H., and Nes, W.R. (1981). The sterols and fatty acids from purified flagella of Chlamydomonas reinhardtii. Lipids *16*, 133–136.

Goetz, S.C., and Anderson, K.V. (2010). The primary cilium: a signalling centre during vertebrate development. Nat. Rev. Genet. *11*, 331–344.

Hammond, G.R., and Balla, T. (2015). Polyphosphoinositide binding domains: Key to inositol lipid biology. Biochim. Biophys. Acta *1851*, 746–758.

Hammond, G.R., Fischer, M.J., Anderson, K.E., Holdich, J., Koteci, A., Balla, T., and Irvine, R.F. (2012). PI4P and PI(4,5)P2 are essential but independent lipid determinants of membrane identity. Science *337*, 727–730.

Hammond, G.R., Machner, M.P., and Balla, T. (2014). A novel probe for phosphatidylinositol 4-phosphate reveals multiple pools beyond the Golgi. J. Cell Biol. *205*, 113–126.

Hildebrandt, F., Benzing, T., and Katsanis, N. (2011). Ciliopathies. N. Engl. J. Med. *364*, 1533–1543.

Humbert, M.C., Weihbrecht, K., Searby, C.C., Li, Y., Pope, R.M., Sheffield, V.C., and Seo, S. (2012). ARL13B, PDE6D, and CEP164 form a functional network for INPP5E ciliary targeting. Proc. Natl. Acad. Sci. USA *109*, 19691–19696.

Jacoby, M., Cox, J.J., Gayral, S., Hampshire, D.J., Ayub, M., Blockmans, M., Pernot, E., Kisseleva, M.V., Compère, P., Schiffmann, S.N., et al. (2009). INPP5E mutations cause primary cilium signaling defects, ciliary instability and ciliopathies in human and mouse. Nat. Genet. *41*, 1027–1031.

Jin, H., White, S.R., Shida, T., Schulz, S., Aguiar, M., Gygi, S.P., Bazan, J.F., and Nachury, M.V. (2010). The conserved Bardet-Biedl syndrome proteins assemble a coat that traffics membrane proteins to cilia. Cell 141, 1208–1219.

Johnson, C.M., Chichili, G.R., and Rodgers, W. (2008). Compartmentalization of phosphatidylinositol 4,5-bisphosphate signaling evidenced using targeted phosphatases. J. Biol. Chem. 283, 29920–29928.

Jonah, M., and Erwin, J.A. (1971). The lipids of membraneous cell organelles isolated from the ciliate, Tetrahymena pyriformis. Biochim. Biophys. Acta 231, 80–92.

Kaneshiro, E.S., Matesic, D.F., and Jayasimhulu, K. (1984). Characterizations of six ethanolamine sphingophospholipids from Paramecium cells and cilia. J. Lipid Res. 25, 369–377.

Kennedy, K.E., and Thompson, G.A., Jr. (1970). Phosphonolipids: localization in surface membranes of Tetrahymena. Science 168, 989–991.

Liem, K.F., Jr., Ashe, A., He, M., Satir, P., Moran, J., Beier, D., Wicking, C., and Anderson, K.V. (2012). The IFT-A complex regulates Shh signaling through cilia structure and membrane protein trafficking. J. Cell Biol. 197, 789–800.

Lin, Y.C., Niewiadomski, P., Lin, B., Nakamura, H., Phua, S.C., Jiao, J., Levchenko, A., Inoue, T., Rohatgi, R., and Inoue, T. (2013). Chemically inducible diffusion trap at cilia reveals molecular sieve-like barrier. Nat. Chem. Biol. 9, 437–443.

Luo, N., West, C.C., Murga-Zamalloa, C.A., Sun, L., Anderson, R.M., Wells, C.D., Weinreb, R.N., Travers, J.B., Khanna, H., and Sun, Y. (2012). OCRL localizes to the primary cilium: a new role for cilia in Lowe syndrome. Hum. Mol. Genet. 21, 3333–3344.

Luo, N., Kumar, A., Conwell, M., Weinreb, R.N., Anderson, R., and Sun, Y. (2013). Compensatory role of inositol 5-phosphatase INPP5B to OCRL in primary cilia formation in oculocerebrorenal syndrome of Lowe. PLoS ONE 8, e66727.

Montesano, R. (1979). Inhomogeneous distribution of filipin-sterol complexes in the ciliary membrane of rat tracheal epithelium. Am. J. Anat. 156, 139–145.

Mukhopadhyay, S., and Jackson, P.K. (2011). The tubby family proteins. Genome Biol. 12, 225.

Mukhopadhyay, S., Wen, X., Chih, B., Nelson, C.D., Lane, W.S., Scales, S.J., and Jackson, P.K. (2010). TULP3 bridges the IFT-A complex and membrane phosphoinositides to promote trafficking of G protein-coupled receptors into primary cilia. Genes Dev. 24, 2180–2193.

Mukhopadhyay, S., Wen, X., Ratti, N., Loktev, A., Rangell, L., Scales, S.J., and Jackson, P.K. (2013). The ciliary G-protein-coupled receptor Gpr161 negatively regulates the Sonic hedgehog pathway via cAMP signaling. Cell 152, 210–223.

Norman, R.X., Ko, H.W., Huang, V., Eun, C.M., Abler, L.L., Zhang, Z., Sun, X., and Eggenschwiler, J.T. (2009). Tubby-like protein 3 (TULP3) regulates patterning in the mouse embryo through inhibition of Hedgehog signaling. Hum. Mol. Genet. 18, 1740–1754.

Patterson, V.L., Damrau, C., Paudyal, A., Reeve, B., Grimes, D.T., Stewart, M.E., Williams, D.J., Siggers, P., Greenfield, A., and Murdoch, J.N. (2009). Mouse hitchhiker mutants have spina bifida, dorso-ventral patterning defects and polydactyly: identification of Tulp3 as a novel negative regulator of the Sonic hedgehog pathway. Hum. Mol. Genet. 18, 1719–1739.

Qin, J., Lin, Y., Norman, R.X., Ko, H.W., and Eggenschwiler, J.T. (2011). Intraflagellar transport protein 122 antagonizes Sonic Hedgehog signaling and controls ciliary localization of pathway components. Proc. Natl. Acad. Sci. USA 108, 1456–1461.

Reiter, J.F., and Skarnes, W.C. (2006). Tectonic, a novel regulator of the Hedgehog pathway required for both activation and inhibition. Genes Dev. 20, 22–27.

Roberson, E.C., Dowdle, W.E., Ozanturk, A., Garcia-Gonzalo, F.R., Li, C., Halbritter, J., Elkhartoufi, N., Porath, J.D., Cope, H., Ashley-Koch, A., et al. (2015). TMEM231, mutated in orofaciodigital and Meckel syndromes, organizes the ciliary transition zone. J. Cell Biol. 209, 129–142.

Rohatgi, R., Milenkovic, L., and Scott, M.P. (2007). Patched1 regulates hedgehog signaling at the primary cilium. Science 317, 372–376.

Roth, M.G. (2004). Phosphoinositides in constitutive membrane traffic. Physiol. Rev. 84, 699–730.

Santos, N., and Reiter, J.F. (2014). A central region of Gli2 regulates its localization to the primary cilium and transcriptional activity. J. Cell Sci. 127, 1500–1510.

Sasaki, T., Takasuga, S., Sasaki, J., Kofuji, S., Eguchi, S., Yamazaki, M., and Suzuki, A. (2009). Mammalian phosphoinositide kinases and phosphatases. Prog. Lipid Res. 48, 307–343.

Smith, J.D., Snyder, W.R., and Law, J.H. (1970). Phosphonolipids in Tetrahymena cilia. Biochim. Biophys. Res. Commun. 39, 1163–1169.

Souto-Padrón, T., and de Souza, W. (1983). Freeze-fracture localization of filipin-cholesterol complexes in the plasma membrane of Trypanosoma cruzi. J. Parasitol. 69, 129–137.

Stauffer, T.P., Ahn, S., and Meyer, T. (1998). Receptor-induced transient reduction in plasma membrane PtdIns(4,5)P2 concentration monitored in living cells. Curr. Biol. 8, 343–346.

Suh, B.C., Inoue, T., Meyer, T., and Hille, B. (2006). Rapid chemically induced changes of PtdIns(4,5)P2 gate KCNQ ion channels. Science 314, 1454–1457.

Tran, P.V., Haycraft, C.J., Besschetnova, T.Y., Turbe-Doan, A., Stottmann, R.W., Herron, B.J., Chesebro, A.L., Qiu, H., Scherz, P.J., Shah, J.V., et al. (2008). THM1 negatively modulates mouse sonic hedgehog signal transduction and affects retrograde intraflagellar transport in cilia. Nat. Genet. 40, 403–410.

Tsujishita, Y., Guo, S., Stolz, L.E., York, J.D., and Hurley, J.H. (2001). Specificity determinants in phosphoinositide dephosphorylation: crystal structure of an archetypal inositol polyphosphate 5-phosphatase. Cell 105, 379–389.

Tyler, K.M., Fridberg, A., Toriello, K.M., Olson, C.L., Cieslak, J.A., Hazlett, T.L., and Engman, D.M. (2009). Flagellar membrane localization via association with lipid rafts. J. Cell Sci. 122, 859–866.

Ueno, T., Falkenburger, B.H., Pohlmeyer, C., and Inoue, T. (2011). Triggering actin comets versus membrane ruffles: distinctive effects of phosphoinositides on actin reorganization. Sci. Signal. 4, ra87.

Vieira, O.V., Gaus, K., Verkade, P., Fullekrug, J., Vaz, W.L., and Simons, K. (2006). FAPP2, cilium formation, and compartmentalization of the apical membrane in polarized Madin-Darby canine kidney (MDCK) cells. Proc. Natl. Acad. Sci. USA 103, 18556–18561.

Wen, X., Lai, C.K., Evangelista, M., Hongo, J.A., de Sauvage, F.J., and Scales, S.J. (2010). Kinetics of hedgehog-dependent full-length Gli3 accumulation in primary cilia and subsequent degradation. Mol. Cell. Biol. 30, 1910–1922.

Yavari, A., Nagaraj, R., Owusu-Ansah, E., Folick, A., Ngo, K., Hillman, T., Call, G., Rohatgi, R., Scott, M.P., and Banerjee, U. (2010). Role of lipid metabolism in smoothened derepression in hedgehog signaling. Dev. Cell 19, 54–65.

Note Added in Proof

Recent work reveals that Inpp5e also controls ciliary phosphoinositide levels and ciliary composition in neural progenitor cells: Chávez, M., Ena, S., Van Sande, J., de Kerchove d'Exaerde, A., Schurmans, A., and Schiffmann, S.N. (2015). Modulation of ciliary phosphoinositide content regulates trafficking and Sonic Hedgehog signaling output. Dev. Cell 34, 338–350.

Phosphoinositides Regulate Ciliary Protein

Trafficking to Modulate Hedgehog Signaling

Francesc R. Garcia-Gonzalo, Siew Cheng Phua, Elle C. Roberson, Galo Garcia III, Monika Abedin, Stéphane Schurmans, Takanari Inoue, and Jeremy F. Reiter

SUPPLEMENTAL FIGURES

Figure S1 (related to Fig.1).

PI(4)P and PI(4,5)P2 localize to distinct ciliary compartments. (**A**) Ciliated IMCD3 cells were stained with anti-PI(4)P (green) and anti-Arl13b (red) antibodies and their nuclei marked with DAPI (blue). Scale bar, 5μm. (**B**) Purified cilia from sea urchin gastrulae were stained with anti-PI(4)P (red) and anti-detyrosinated tubulin (Glu-Tub, green) antibodies. Scale bar, 5μm. (**C**) Live IMCD3 cells were imaged for the ciliary marker 5HT6-CFP (red) and the PI(4,5)P_2 sensor EYFP-PH$^{PLC\delta1}$ (green). Scale bar, 5μm. (**D**) XZ optical section of live IMCD3 cells expressing 5HT6-CFP (red) and EYFP-PH$^{PLC\delta1}$ (green). Scale bar, 5μm. (**E**) Live imaging of NIH-3T3 cells cotransfected with plasmids expressing the PI(4,5)P2 sensor mCerulean3-PH$^{PLC\delta1}$ (green) and the indicated ciliary fusion proteins (red) containing the catalytically active and inactive forms of Inp54p, a yeast PI(4,5)P_2 5-phosphatase, and PIPK, a mouse PI(4)P 5-kinase. Scale bars, 5μm. (**F**) Quantitation of the extension of the mCerulean3-PH$^{PLC\delta1}$ flurorescence relative to ciliary length. The catalytically active phosphatase and kinase decreased and increased, respectively, the extent of ciliary mCerulean3-PH$^{PLC\delta1}$ flurorescence. Data are means ± standard error of the mean (SEM). Asterisks indicate p<0.05 in unpaired t-tests.

Figure S2 (related to Fig.2).

Inpp5e and Tctn1 affect ciliary PI(4,5)P_2 levels. (**A**) MEFs derived from littermate *Inpp5e*$^{+/-}$ and *Inpp5e*$^{-/-}$ embryos were stained for Tub^{Ac} (red), Inpp5e (green), γ-Tub (cyan) and DNA (blue). Scale bar, 5μm. (**B**) *Inpp5e*$^{+/-}$ and *Inpp5e*$^{-/-}$ MEFs were starved for 48 hours and stained for Tub^{Ac} (green), Arl13b (red), and DNA (blue). Scale bar, 5μm. (**C**) Quantitation

of the proportion of *Inpp5e*$^{+/-}$ and *Inpp5e*$^{-/-}$ MEFs that possessed cilia. Error bars depict standard deviations (SDs). (**D**) Live imaging of *Inpp5e*$^{-/-}$ MEFs cotransfected with plasmids expressing the PI(4,5)P$_2$ sensor mCerulean3-PH$^{PLC\delta1}$ (green) and the indicated ciliary fusion proteins (red) of catalytically inactive (D281A) or wild type Inp54p, a yeast PI(4,5)P$_2$ 5-phosphatase. Scale bars, 5μm. Quantitation of the extent of ciliary mCerulean3-PH$^{PLC\delta1}$ fluorescence (PI(4,5)P$_2$ length) relative to the cilium length in *Inpp5e*$^{-/-}$ MEFs. Data are means ± SEM. Asterisks indicate p<0.01 in unpaired t-tests. (**E**) Live *Tctn1*$^{+/+}$ and *Tctn1*$^{-/-}$ MEFs were imaged for the ciliary marker 5HT6-CFP (red) and the PI(4,5)P$_2$ sensor EYFP-PH$^{PLC\delta1}$ (green). Scale bars, 5μm. (**F**) Quantitation of the extent of ciliary EYFP-PH$^{PLC\delta1}$ fluorescence (PI(4,5)P$_2$ length) relative to the extent of 5HT$_6$-CFP fluorescence (Cilium length) in *Tctn1*$^{+/+}$ and *Tctn1*$^{-/-}$ MEFs. Data are means ± SEM. Asterisks indicate p<0.01 in unpaired t-tests.

Figure S3 (related to Fig.3).

Inpp5e regulates Hh signaling. (**A**) qRT-PCR quantitation of *Gli1* expression by *Inpp5e*$^{+/-}$ and *Inpp5e*$^{-/-}$ MEFs treated with vehicle (DMSO), SAG or ShhN. Data are means ± SDs from triplicates of one experiment. (**B**) qRT-PCR quantitation of *Ptch1* expression by *Inpp5e*$^{+/-}$ and *Inpp5e*$^{-/-}$ MEFs treated with vehicle (DMSO), SAG or ShhN. Data are means ± SDs from triplicates of one experiment. (**C**) Fold induction of *Ptch1* and *Gli1* expression by SAG relative to vehicle (DMSO) in *Inpp5e*$^{+/-}$ and *Inpp5e*$^{-/-}$ MEFs. Asterisks indicate p<0.01 in unpaired t-tests. (**D**) *Inpp5e*$^{+/-}$ and *Inpp5e*$^{-/-}$ MEFs were stained for Tub^{Ac} (red), Ptch1 (green) and DNA (blue). Arrows indicate ciliary Ptch1. Insets depict magnified view of a single cilium. Scale bar, 5μm. (**E**) *Inpp5e*$^{+/-}$ and *Inpp5e*$^{-/-}$ MEFs were stained for Tub^{Ac} (red),

Polycystin-2 (green) and DNA (blue). Arrows indicate ciliary Polycystin-2. Insets depict magnified view of a single cilium. Scale bar, 5μm. (**F**) Fold increase in ciliary Smo by SAG relative to vehicle in *Inpp5e*$^{+/-}$ and *Inpp5e*$^{-/-}$ MEFs. (**G**) Fold increase in Gli3 at the ciliary tip by SAG relative to vehicle in *Inpp5e*$^{+/-}$ and *Inpp5e*$^{-/-}$ MEFs. Asterisk indicates p<0.05 in unpaired t-test. (**H**) Fold reduction in ciliary Gpr161 levels by SAG relative to vehicle in *Inpp5e*$^{+/-}$ and *Inpp5e*$^{-/-}$ MEFs.

Figure S4 (related to Fig.4).

Inpp5e regulates IFT-A but not IFT-B ciliary localization. (**A**) *Inpp5e*$^{+/-}$ and *Inpp5e*$^{-/-}$ MEF lysates were blotted for Tulp3 (top) and α-Tubulin (bottom). Molecular weight markers are shown in the left. (**B**) *Inpp5e*$^{+/-}$ and *Inpp5e*$^{-/-}$ MEFs were stained for Tub^{Ac} (green), Ift139 (red), γ-Tub (cyan), and DNA (blue). Scale bar, 5μm. Insets depict magnified view of a single cilium. (**C**) Ventral neural tube sections of E9.5 *Inpp5e*$^{+/-}$ and *Inpp5e*$^{-/-}$ mouse embryos were stained for Arl13b (red), γ-Tub (cyan), Ift88 (green), and DNA (blue). Ventral is down. Insets depict magnified view of cilia. Scale bar, 5μm. (**D**) *Tctn1*$^{+/+}$ and *Tctn1*$^{-/-}$ MEFs were stained for Tub^{Ac} (green), Tulp3 (red), γ-Tub (cyan), and DNA (blue). Scale bar, 5μm. (**E**) *Tctn1*$^{+/+}$ and *Tctn1*$^{-/-}$ MEFs were stained for Tub^{Ac} (green), Gpr161 (red), γ-Tub (cyan), and DNA (blue). Scale bar, 5μm.

Figure S5 (related to Fig.5).

Ciliary PI(4,5)P$_2$ synthesis increases ciliary Gpr161 levels. (**A**) IMCD3 cells expressing wild type (WT) or catalytically inactive (D253A) 5-HT$_6$-EYFP-PIPK were stained for Tub^{Ac} (cyan), EYFP (green) and Gpr161 (red). Arrowheads indicate 5-HT$_6$-EYFP-PIPK-containing

cilia. Scale bar, 5μm. (**B**) Quantification of the fluorescence intensity of Gpr161 in cilia expressing 5-HT$_6$-EYFP-PIPK WT or D253A. Data are means ± SEM. Asterisk indicates p<0.05 in unpaired t-test.

Figure S6 (related to Fig.6).

Inhibiting Tulp3 or Gpr161 increases Hh signaling in *Inpp5e*$^{-/-}$ cells. (**A**) *Inpp5e*$^{-/-}$ MEFs transfected with *Tulp3* siRNA (*siTulp3*), *Gpr161* siRNA (*siGpr161*) or scrambled control siRNA (*siCtrl*) were stained for Tulp3 or Gpr161 (green), Tub^{Ac} (red), γTub (cyan) and nuclei (blue). Scale bars, 5μm. (**B**) Lysates of *Inpp5e*$^{-/-}$ MEFs transfected with either a scrambled control (*siControl*) or Tulp3 (*siTulp3*) siRNAs were blotted for Tulp3 (top) and α-Tubulin (bottom). Molecular weight markers are shown in the left. (**C**) Quantification of the fluorescence intensity of Tulp3 and Gpr161 in cilia of *siTulp3* or *siGpr161*-transfected *Inpp5e*$^{-/-}$ MEFs relative to *siCtrl*-transfected *Inpp5e*$^{-/-}$ MEFs. Data are means ± SEM. One asterisk indicates p<0.05 and two indicates p<0.01 in unpaired t-tests. (**D**) *Inpp5e*$^{+/-}$ and *Inpp5e*$^{-/-}$ MEFs transfected with *siTulp3, siGpr161* or *siCtrl* were treated with SAG or vehicle and expression of *Ptch1* was measured by qRT-PCR. Error bars represent SDs of three independent experiments. One asterisk indicates p<0.05 and two represents p<0.01 in unpaired t-tests. (**E**) Fold induction of *Ptch1* expression by SAG relative to vehicle in *Inpp5e*$^{+/-}$ and *Inpp5e*$^{-/-}$ MEFs. Data are means ± SEM. One asterisk indicates p<0.05 and two indicates p<0.01 in unpaired t-tests.

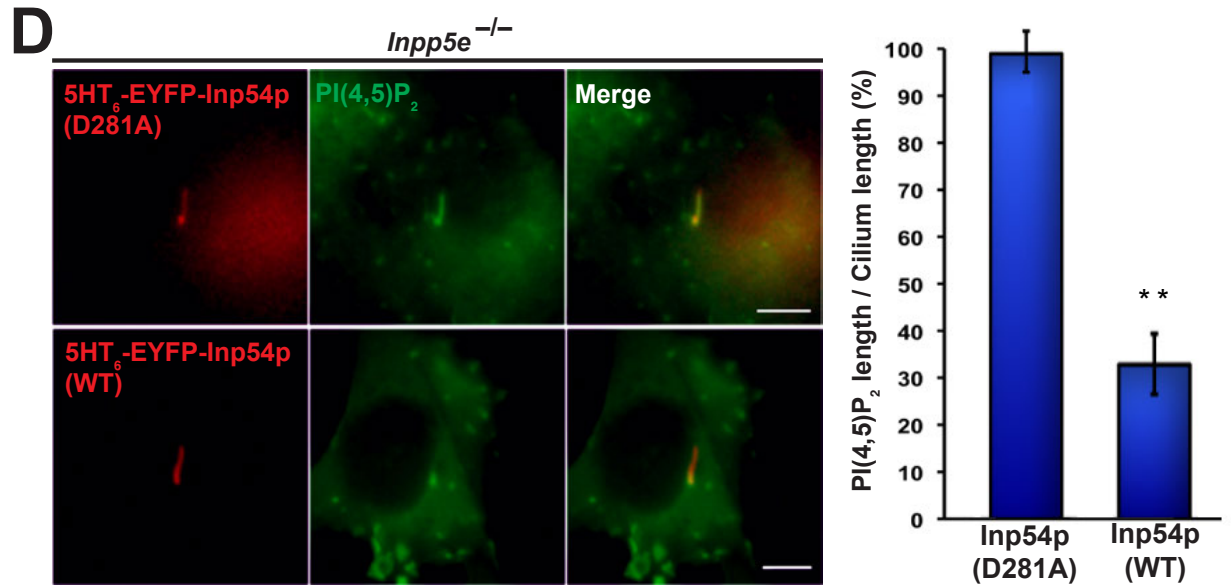# Figure S1. Garcia-Gonzalo et al. 2015
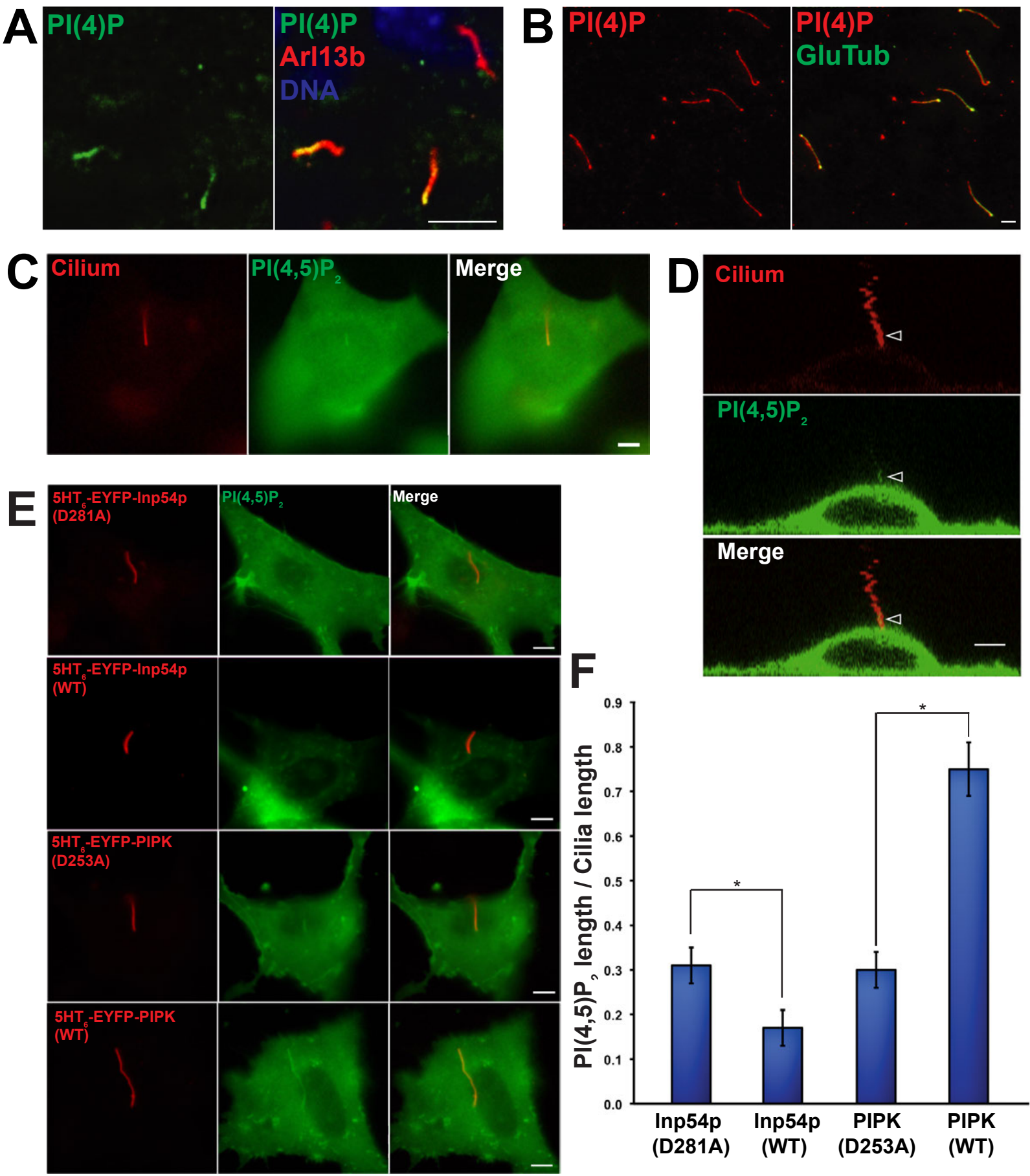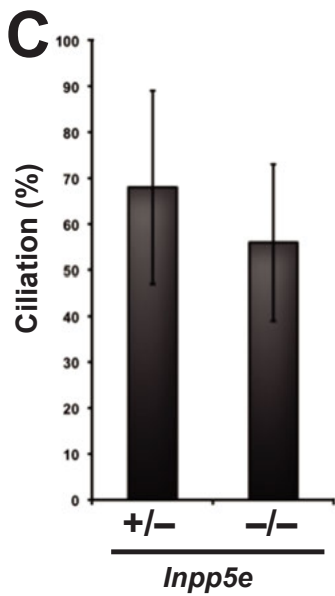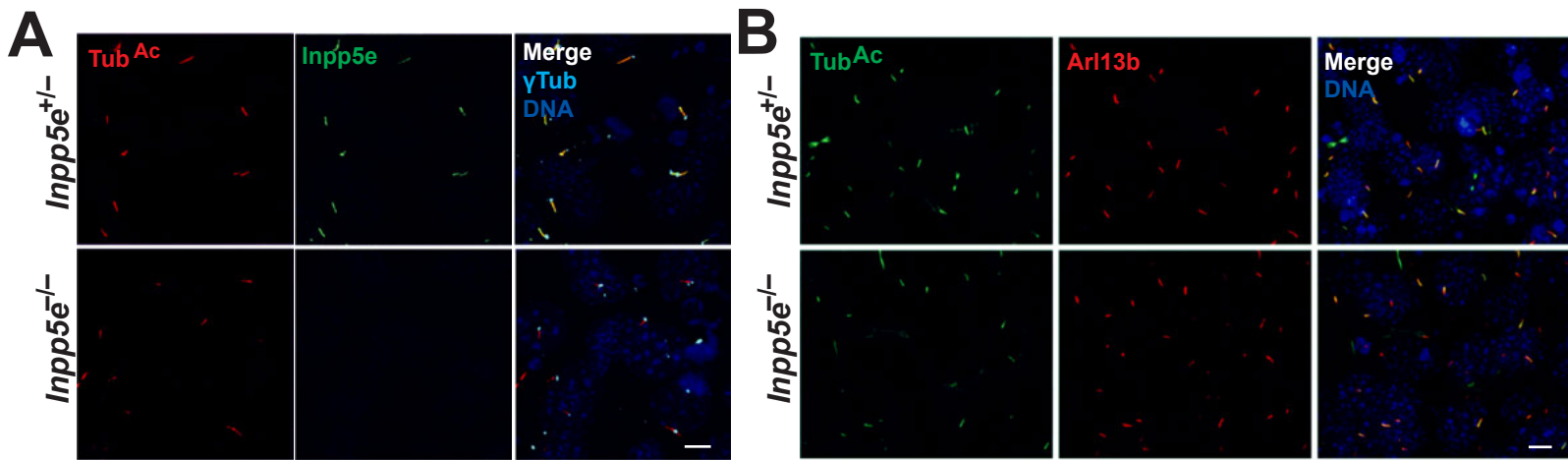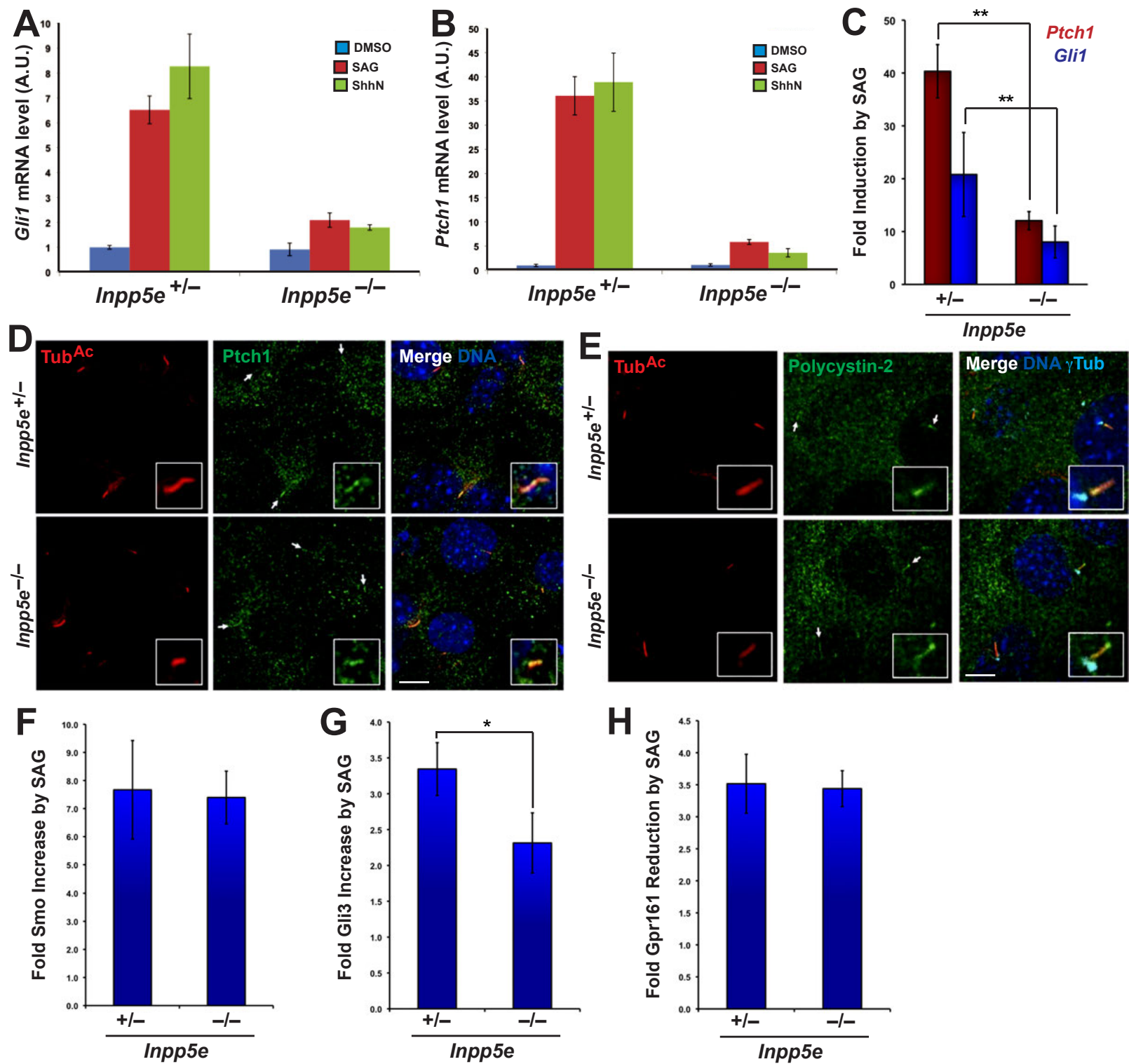
Figure S2. Garcia-Gonzalo et al. 2015
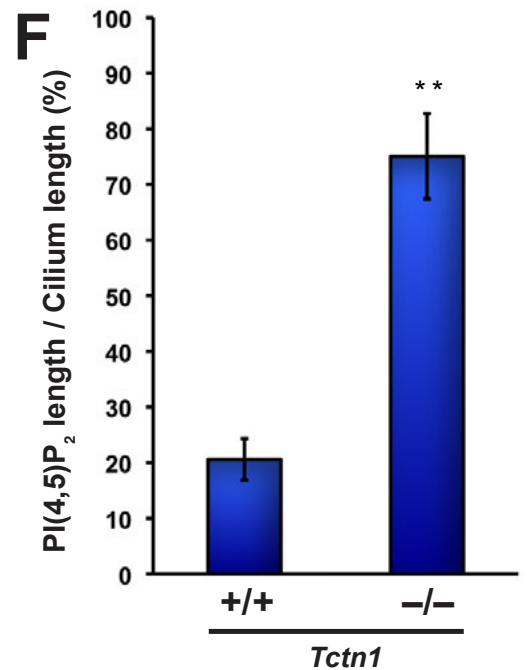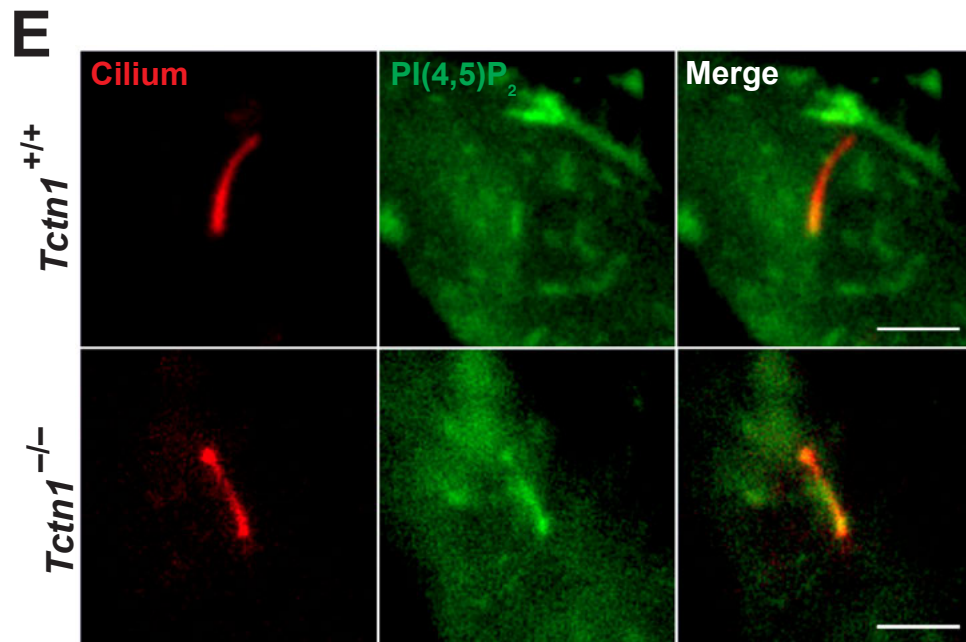
Figure S3. Garcia-Gonzalo et al. 2015
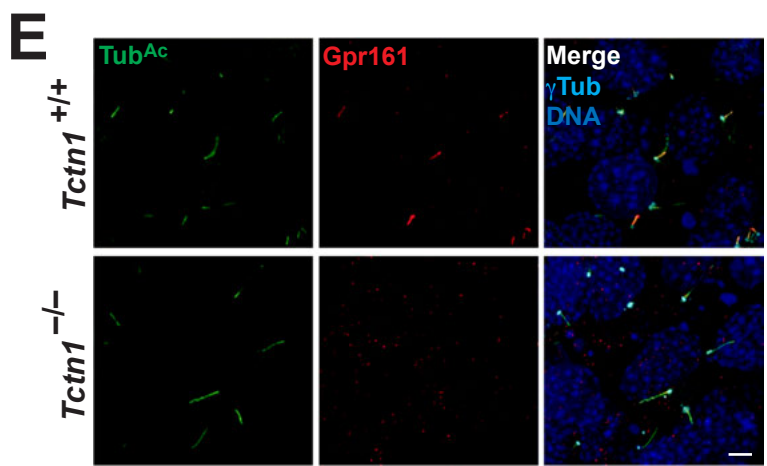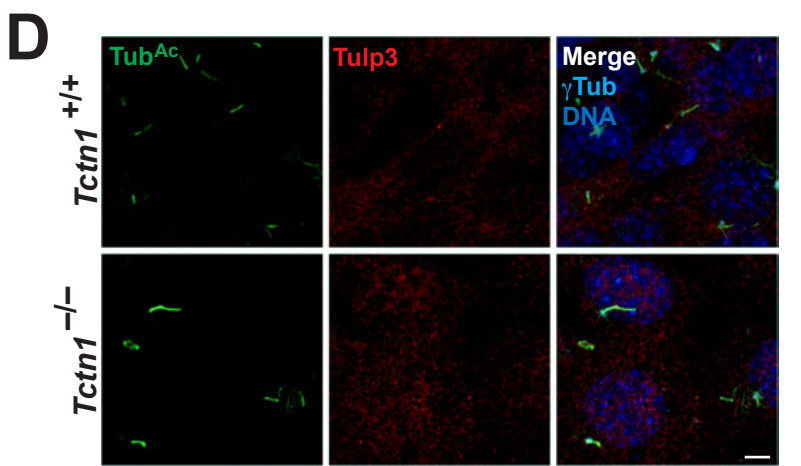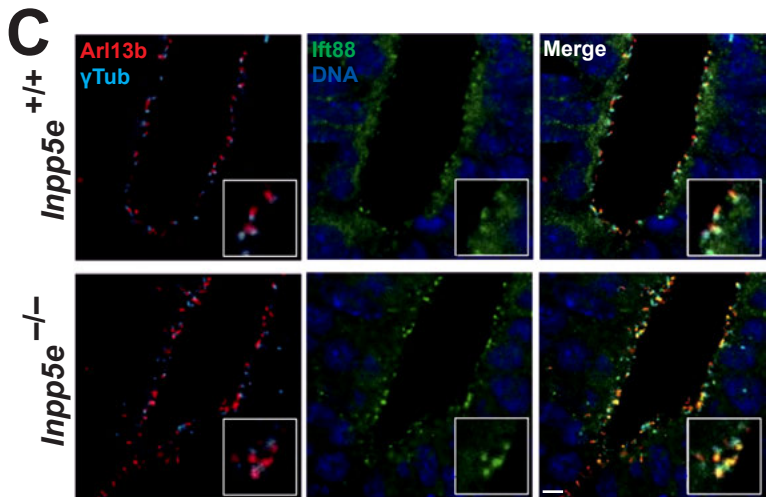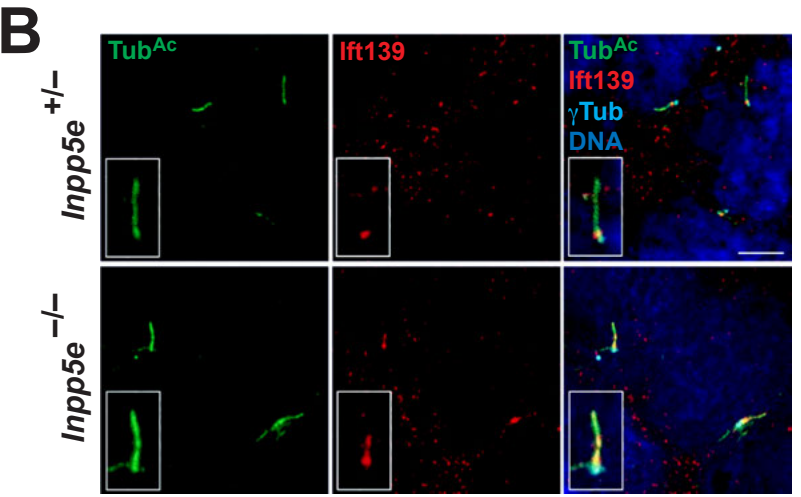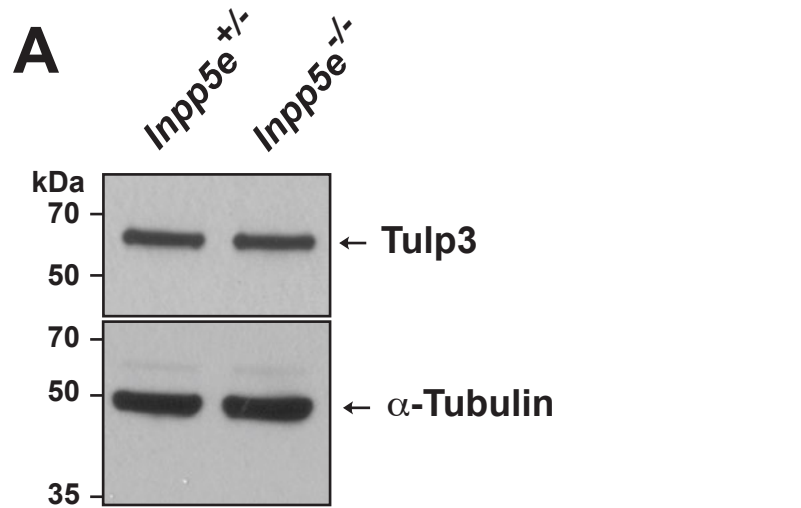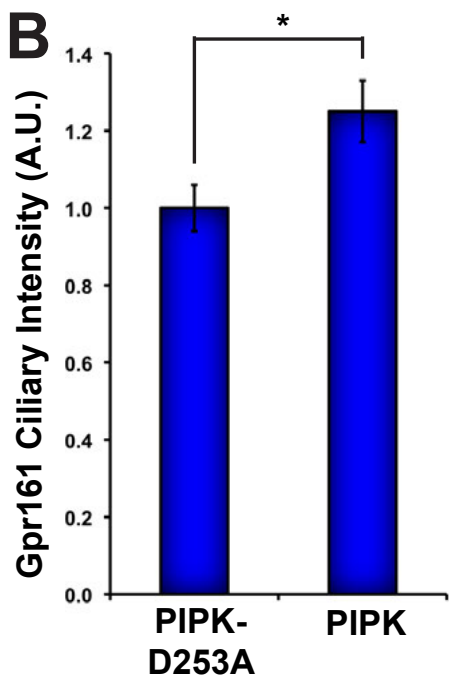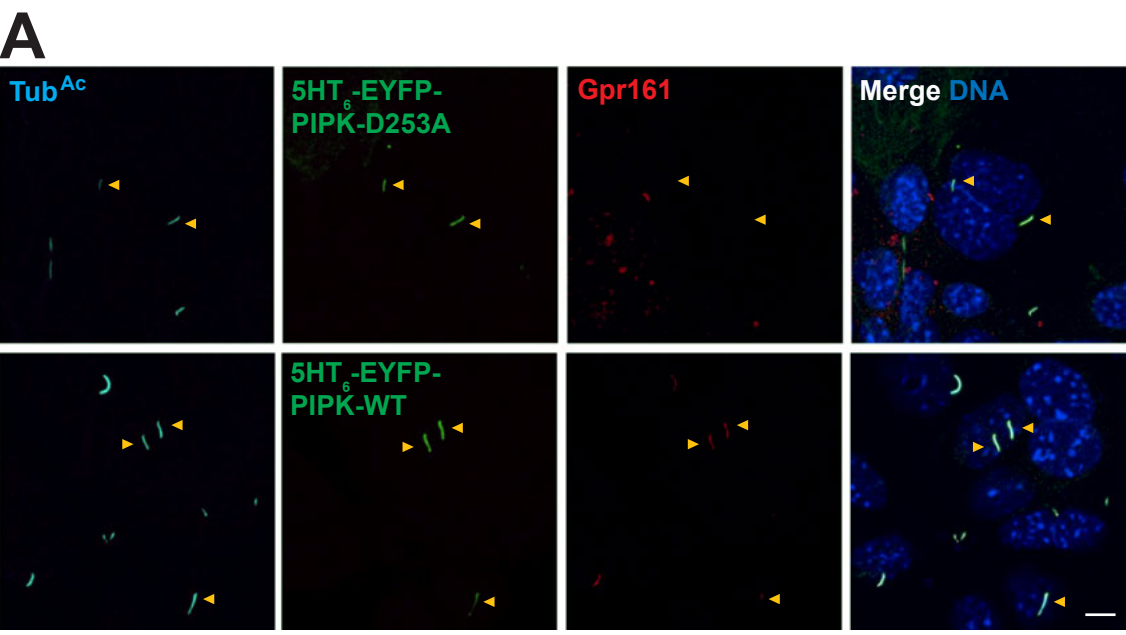
Figure S4. Garcia-Gonzalo et al. 2015

Figure S5. Garcia-Gonzalo et al. 2015

A

B

Figure S6. Garcia-Gonzalo et al. 2015